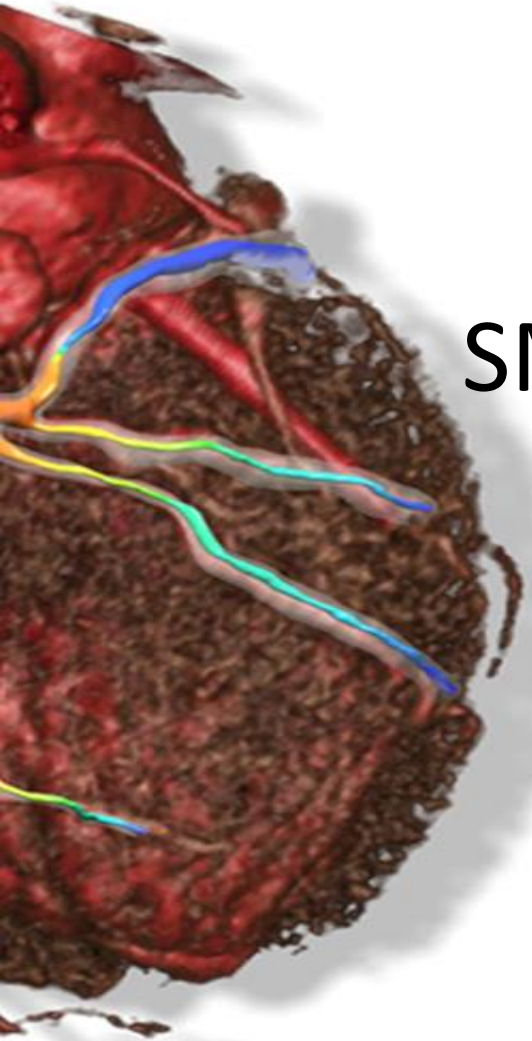


A SMARTool project workshop

# CAD RISK PREDICTION AND STRATIFICATION: THE ICT APPROACH



## SMARTool Imaging Computational Models

Prof. Dimitrios I. Fotiadis

Professor of Biomedical Engineering

Tuesday 6<sup>th</sup> November 2018

CNR Research Area Campus  
Building A, Room 27  
via Moruzzi, 1 Pisa - Italy



Horizon 2020  
689068

# Aims



## Patient-specific CAD stratification

A machine learning based risk stratification model will be implemented by patient genotyping and phenotyping



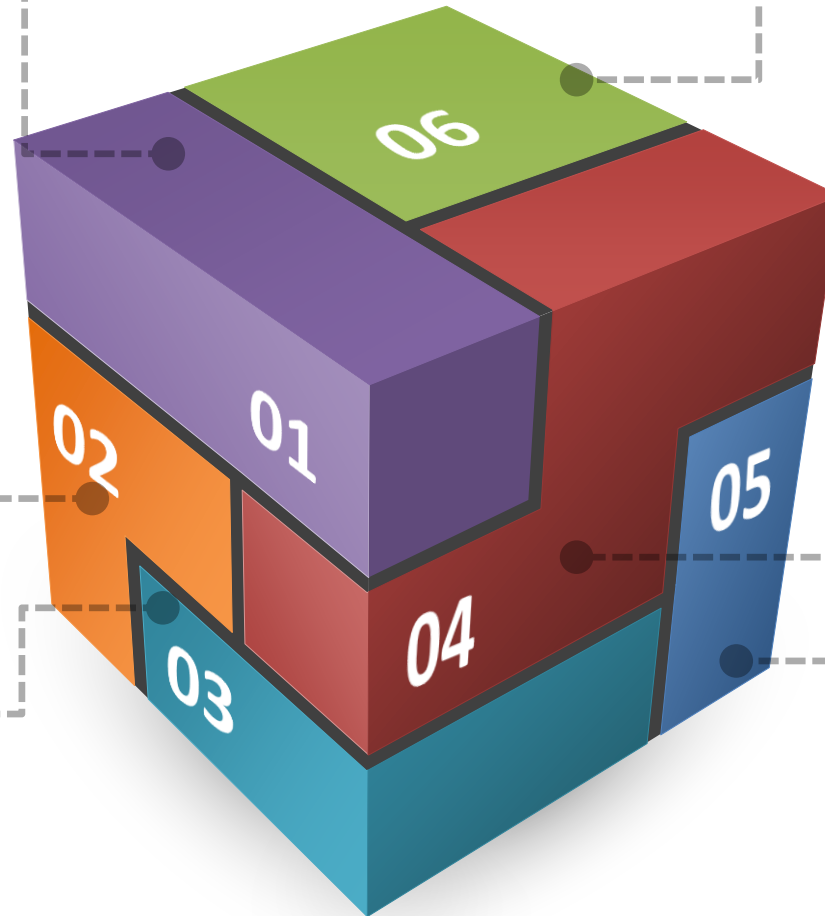
## Patient-specific CAD diagnosis

CAD diagnosis is based on semi-automate 3D arterial reconstruction and non-invasive FFR measurement.



## CAD prognosis decision support

Models of site specific plaque growth and prediction will be implemented for the prediction of regions prone to plaque growth



## Cloud based platform

All outcomes are integrated into a unified cloud based platform



## Treatment decision support

A virtual angioplasty tool will be developed

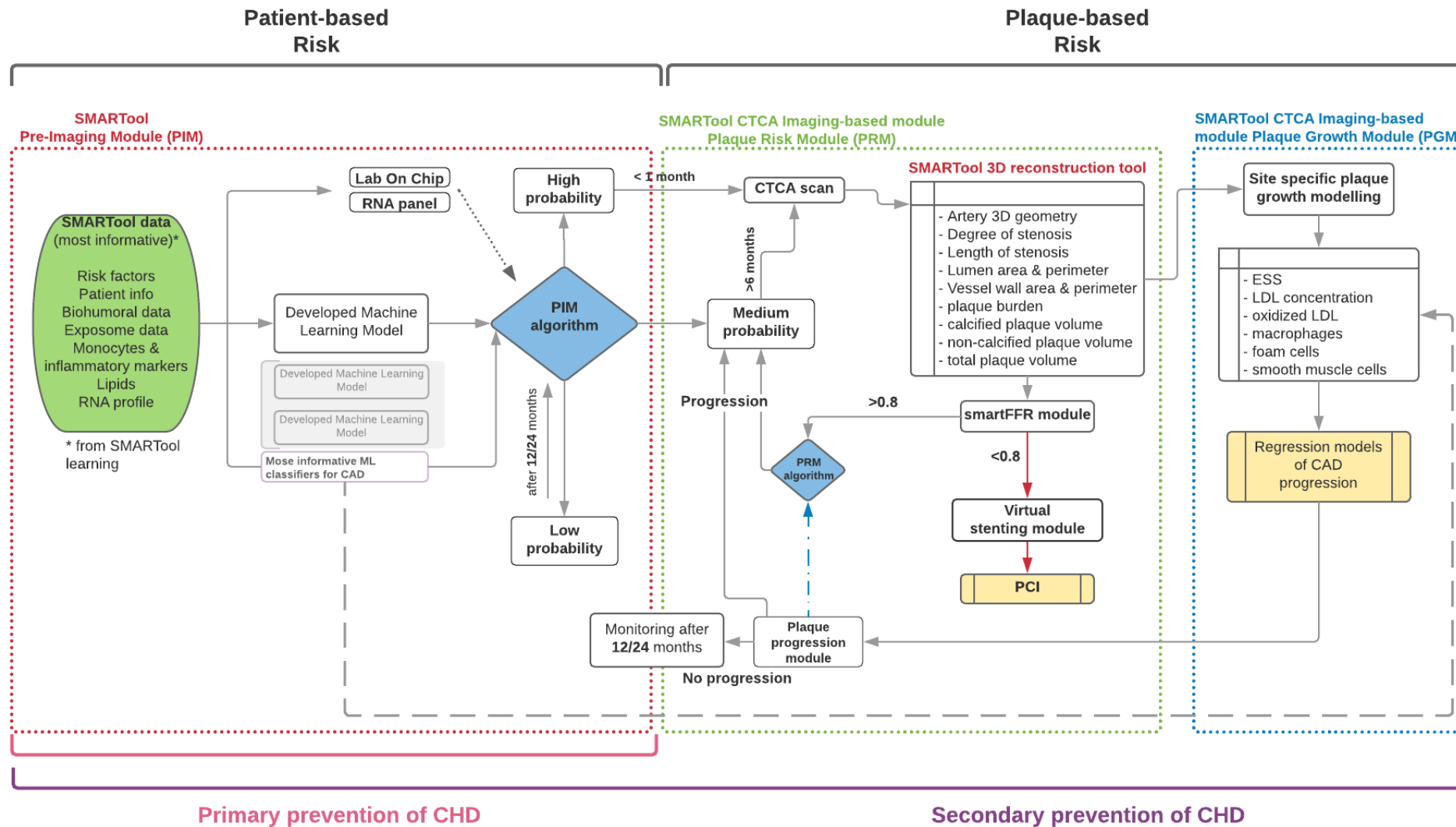


## Point-of-care testing

SMARTool will deliver a microfluidic device for on-chip blood analysis usable in CDSS

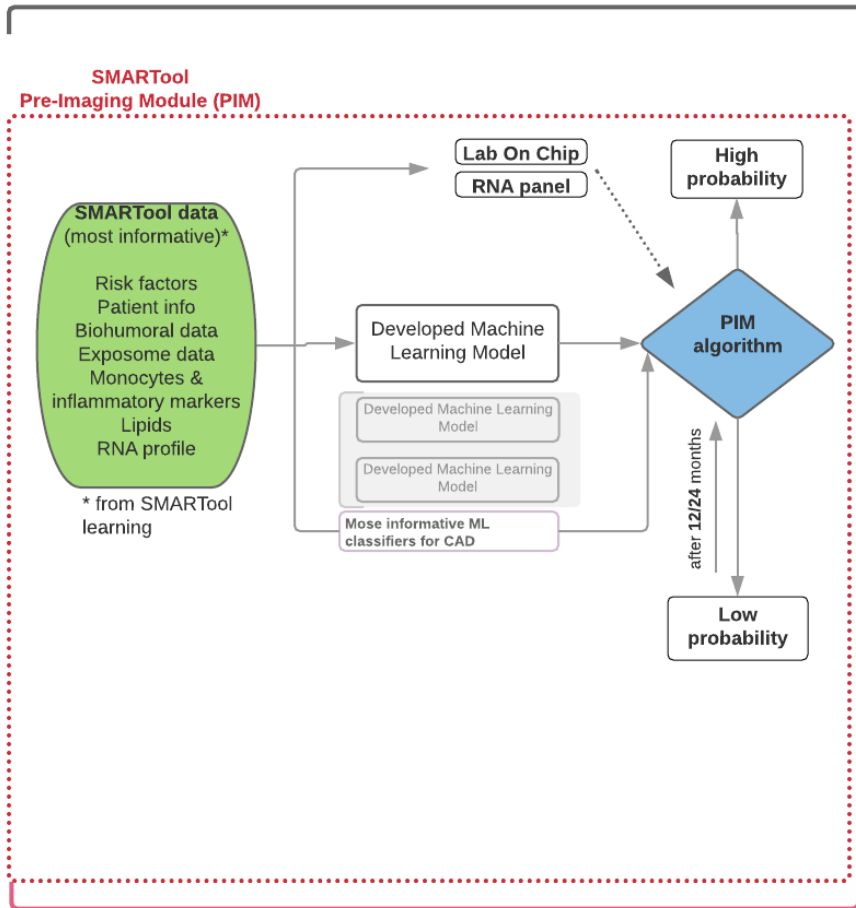


# SMARTool Conceptual Architecture



# SMARTool pre-imaging module (PIM)

## Patient-based Risk



Primary prevention of CHD



To design and develop a machine learning-based model effectively integrating multiple categories of biological non-imaging data towards precise risk stratification in coronary artery disease

To identify the most informative features refining the existing stratification scores with at least 2 novel features

To validate the risk stratification model on retrospective and prospective data annotated using CCTA

# CAD Risk stratification general pipeline

## Data Pre-processing

- Data cleaning
- Feature Ranking

## Machine Learning

- Selection of ML classifier with best performance characteristics
- Linear and non-Linear algorithms

## Model Optimization - Selection

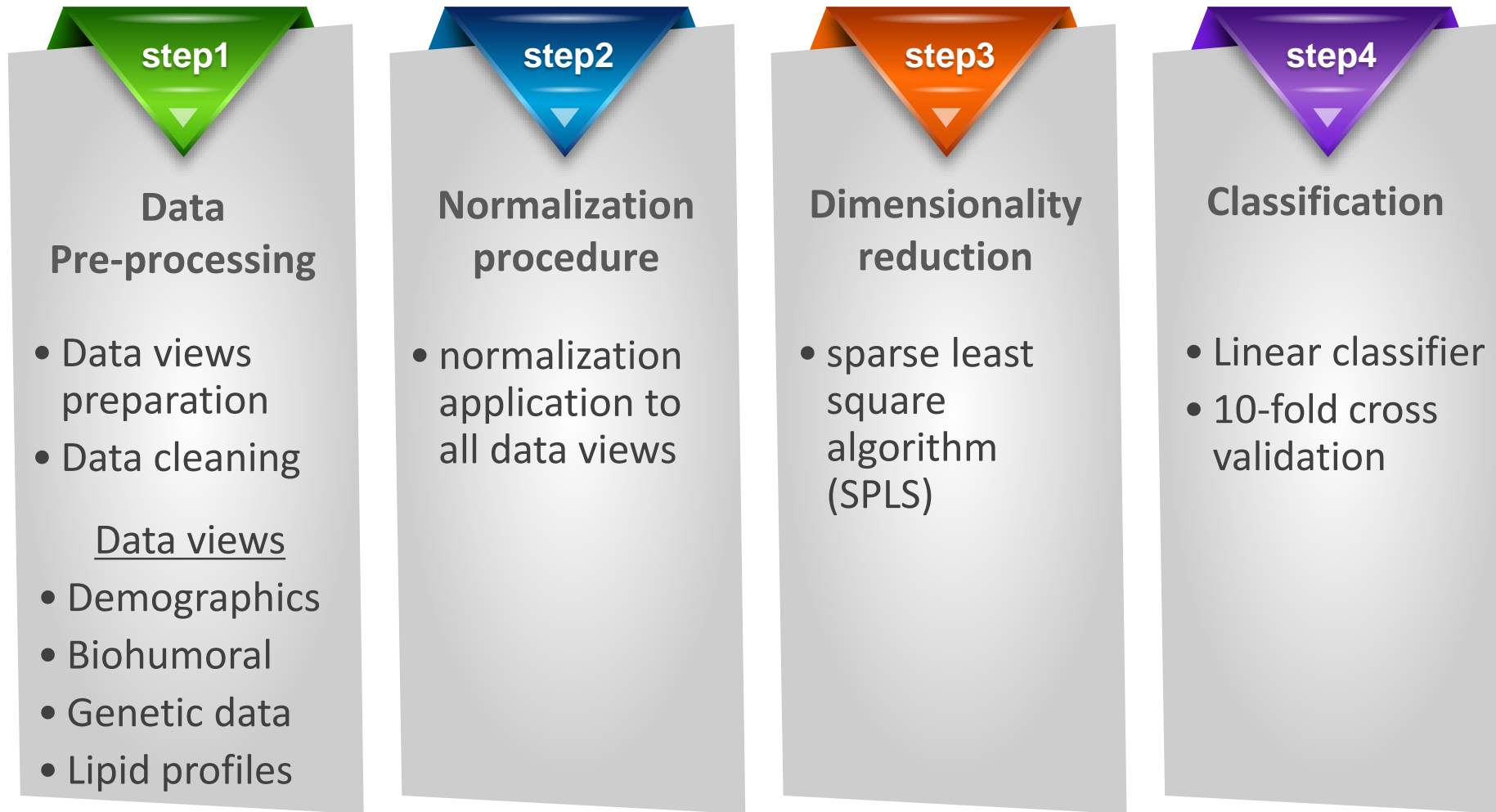
- Hyperparameter optimization on the training set
- Sequential feature selection

## Performance Evaluation

- Repeated 10-fold cross-validation



# CAD Risk stratification specific pipeline for high dimensionality feature set



# Problem formulation

- In SMARTool 3 problem subcase has been defined
  - Subcase 1
    - Class0: No CAD
    - Class1: Obstructive CAD and Severe CAD
  - Subcase 2
    - Class0: No CAD, minimal CAD
    - Class1: Non-Obstructive CAD, Obstructive CAD and Severe CAD
  - Subcase 3
    - Class0: No CAD, minimal CAD
    - Class1: Non-Obstructive CAD
    - Class2: Obstructive CAD and Severe CAD

# Smartool follow-up dataset

- A very comprehensive dataset has been collected including:



## Data Groups

Demographics

Risk Factors

Biohumoral data

Inflammatory and Monocyte  
Markers

Omics Data

Symptoms data

Exposome data



The SMARTool dataset includes 263 subjects



The 210 subjects has genetic data



All of them are annotated from the SMARTool  
Clinical experts



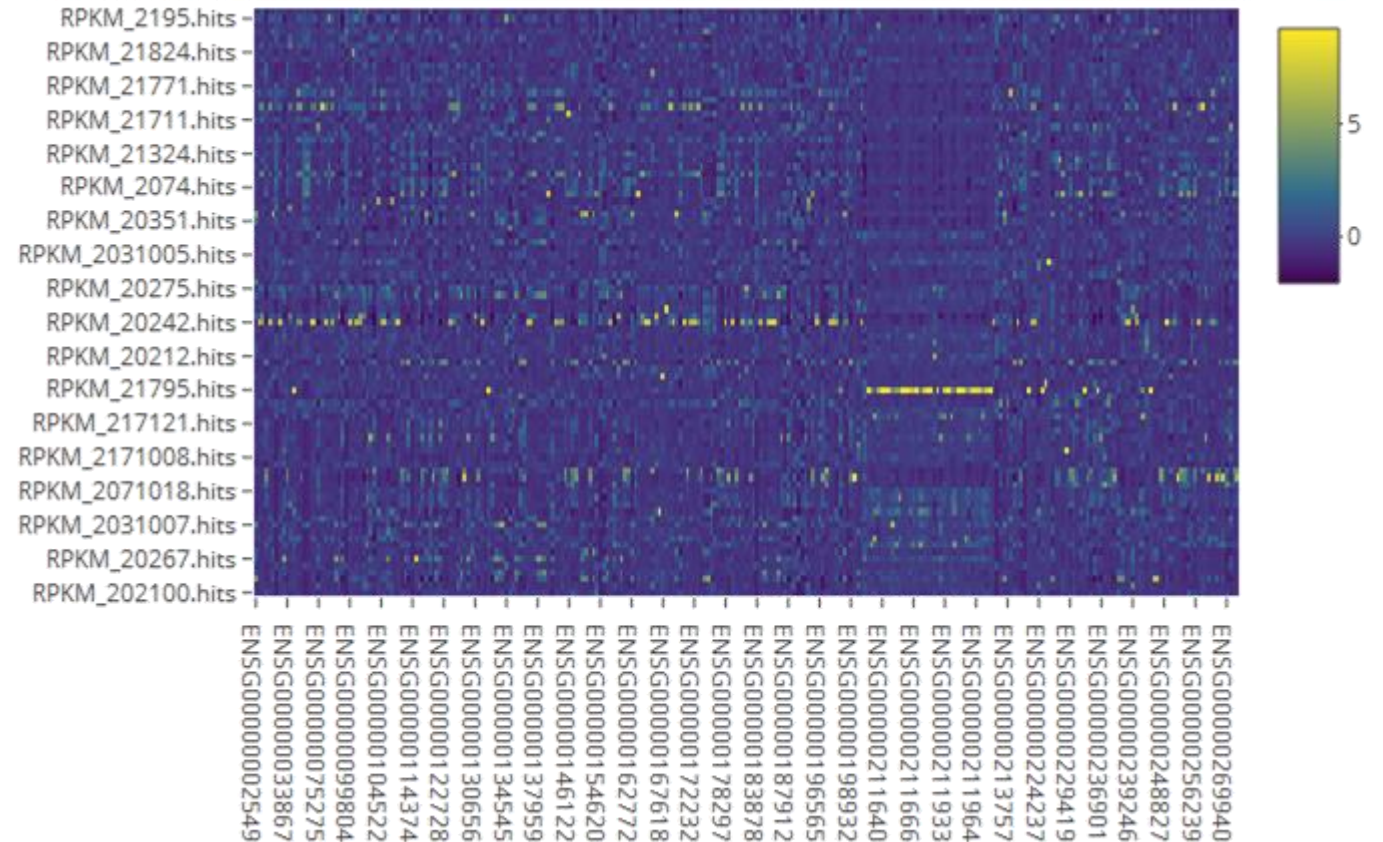
# Statistical data analysis

## Gene Expression Dataset ( $p = 55629$ )

The edgeR analysis identified  $p = 283$  differentially expressed genes.

## Lipids Dataset ( $p = 59$ ) - 1-way ANCOVA

Statistically significant differences in Cer(d18:1/16:0), TG(54:2), TG(18:1/18:1/18:0) M, SM(36:2), SM(38:2), SM(40:2), SM(42:4), SM(42:3) lipids species between the groups, when adjusted for triglycerides and LDL ( $p < .01$ ).



### Exploratory data analysis

Heat map of the expression values (RPKM) of differentially expressed genes between groups

# Evaluation of PIM Classification Performance

Input	Method	Accuracy	Sensitivity	Specificity	PPV	NPV
Age, Gender, Blood Tests, Biohumoral Data, Inflammatory Markers	Logistic regression	0.71±0.19	0.77±0.24	0.63±0.32	0.76±0.19	0.70±0.26
	Linear discriminant analysis	0.73±0.17	0.77±0.20	0.68±0.34	0.82±0.17	0.65±0.31
Age, Gender, Differentially Expressed Genes	<b>Sparse partial least squares, Logistic regression</b>	<b>0.85±0.14</b>	<b>0.90±0.14</b>	<b>0.77±0.33</b>	<b>0.88±0.16</b>	<b>0.87±0.19</b>
	Sparse partial least squares, Linear discriminant analysis	0.79±0.10	0.86±0.13	0.68±0.26	0.83±0.13	0.80±0.19
Differentially Expressed Genes, Lipids	Sparse generalized canonical correlation analysis, Linear discriminant analysis	0.78±0.10	0.80±0.16	0.75±0.25	0.84±0.14	0.77±0.18

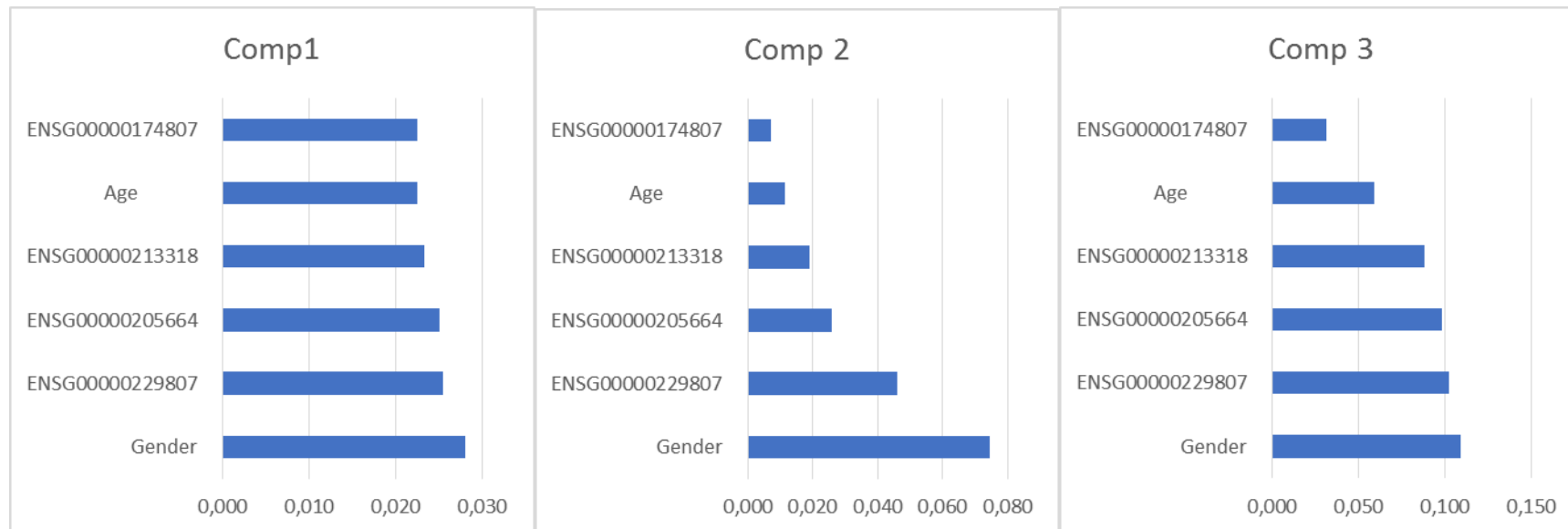
**Evaluation Procedure:** 10-fold cross validation accompanied by an internal 10-fold cross-validation for hyper-parameter tuning .

# Classification performance

## Sparse PLS of demographics and gene expression data

**Evaluation Procedure:** 10-fold cross validation accompanied by an internal 10-fold cross-validation for hyper-parameter tuning .

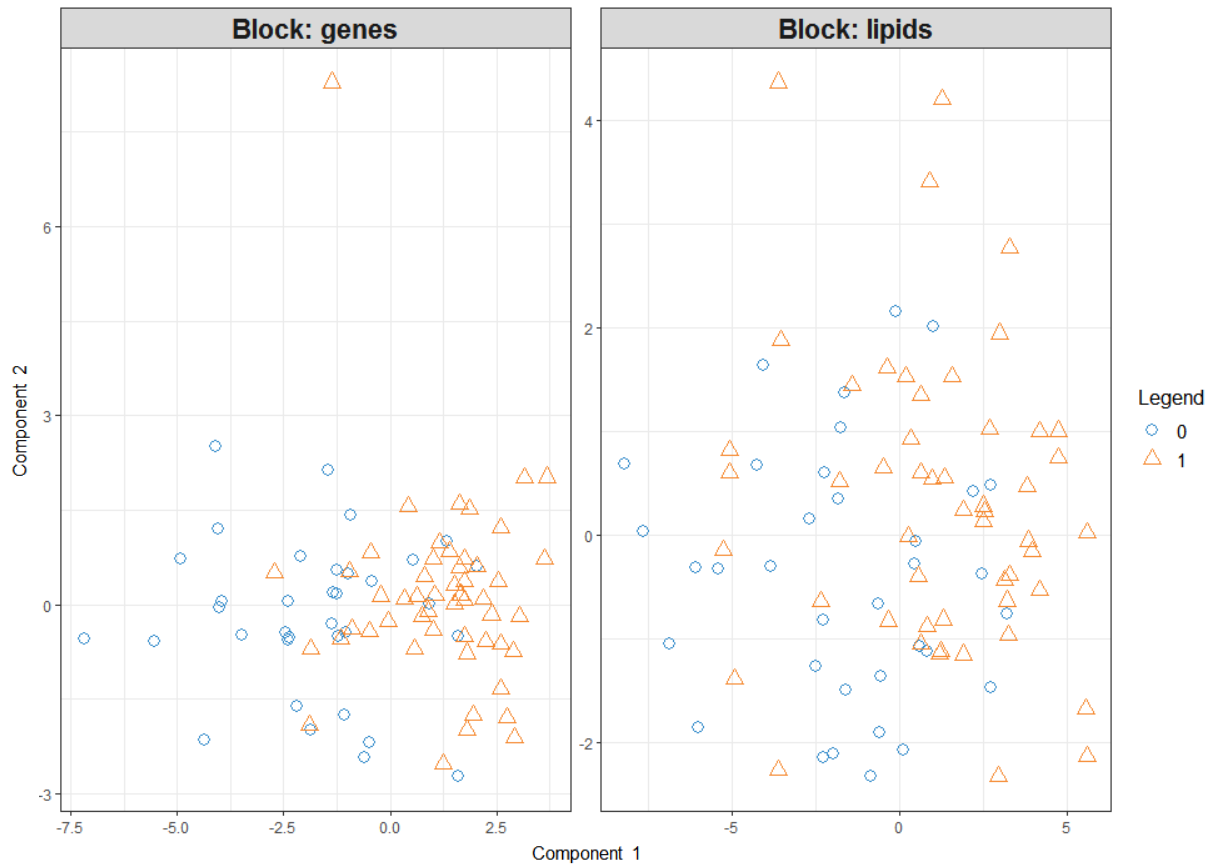
### Selected variables in each of the 3 components ( $K = 3$ )



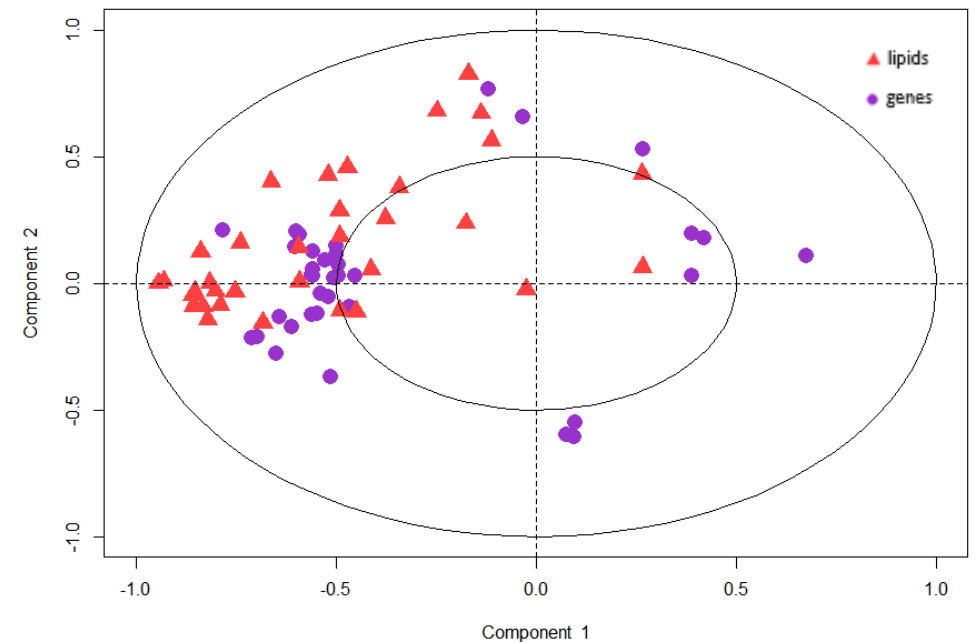
# Output visualization

## Sparse Generalized Canonical Correlation Analysis of Lipids and Genes

Representation of individuals

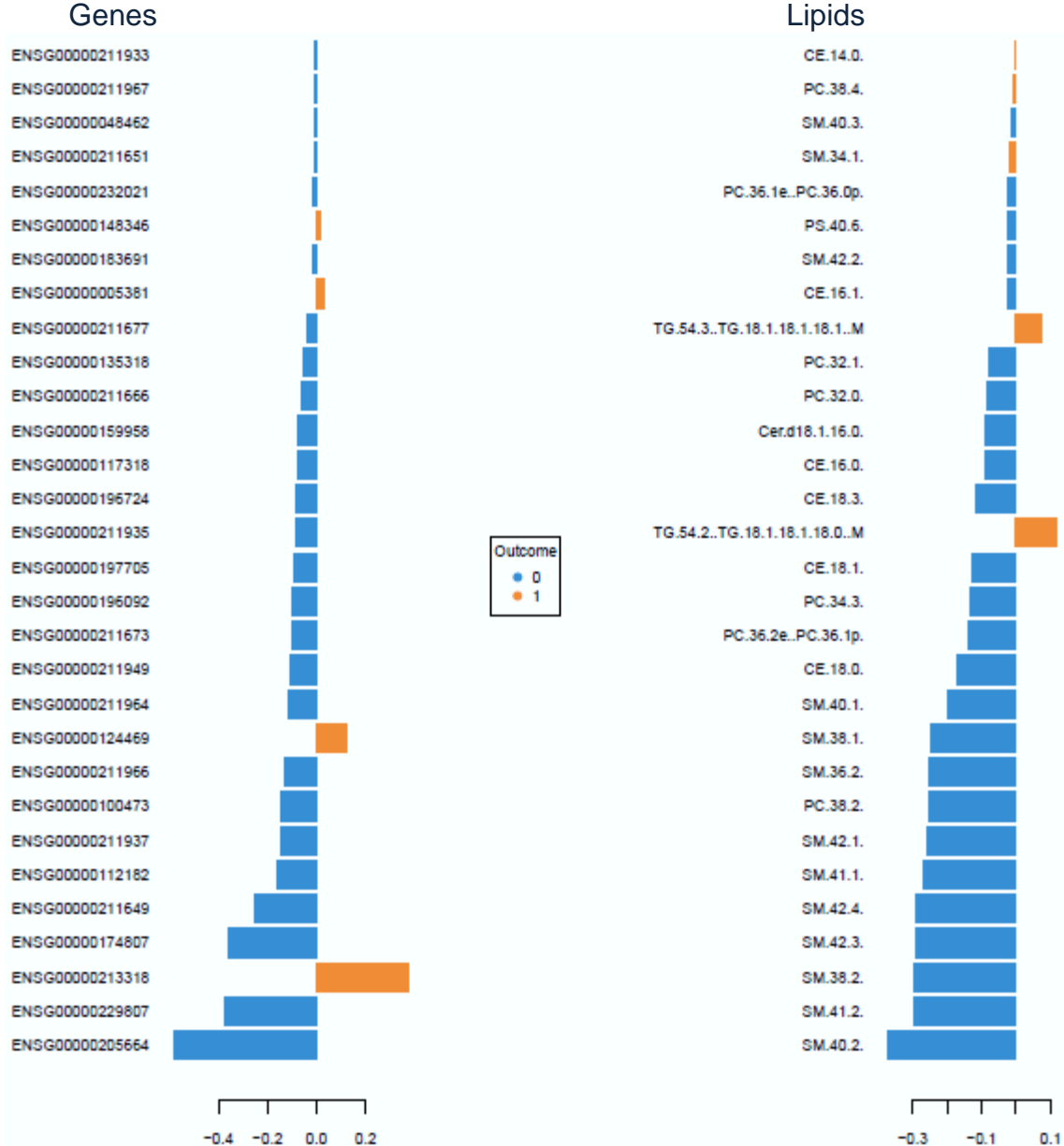


Representation of features

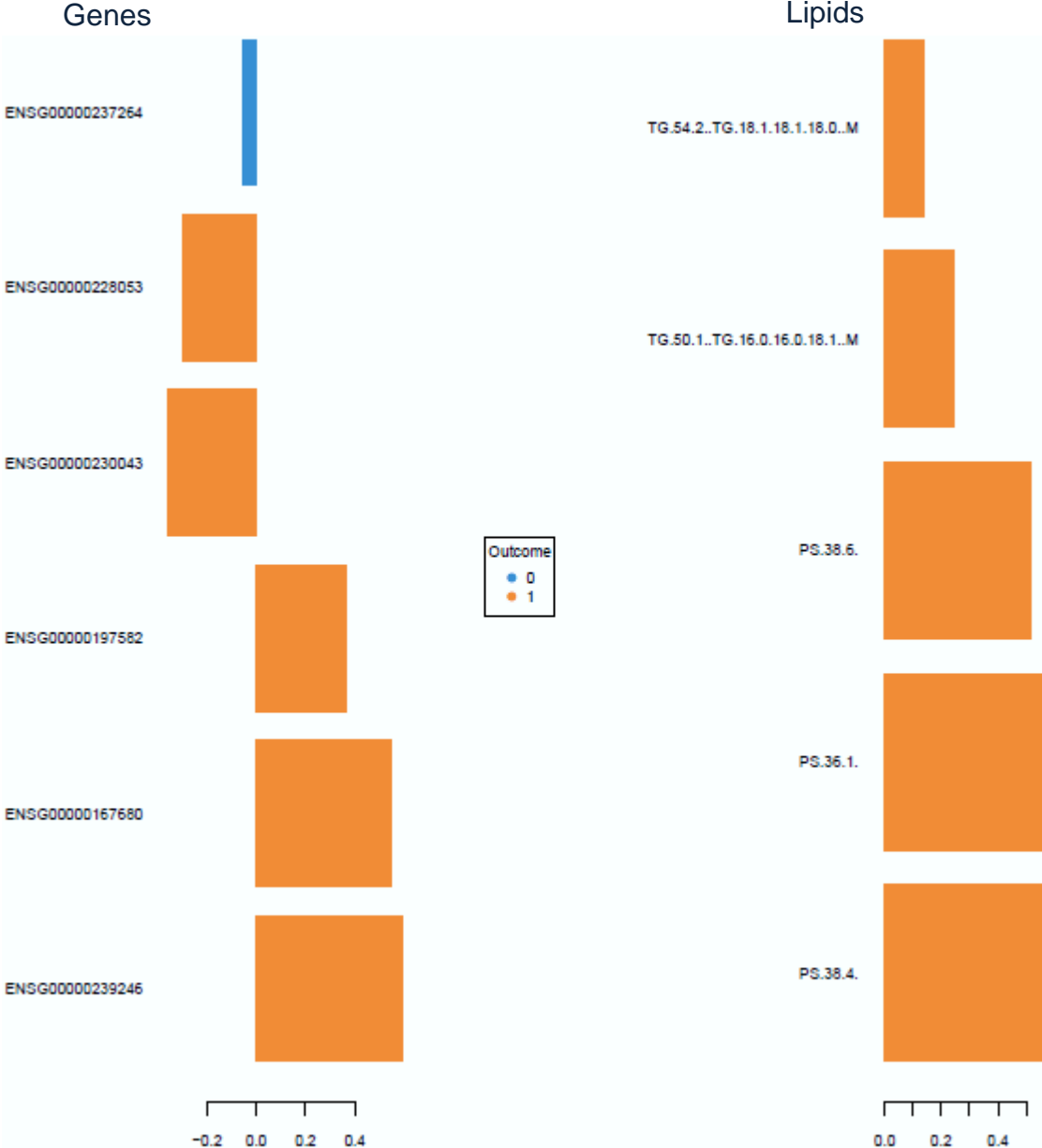


# Sparse Generalized Canonical Correlation Analysis of Lipids and Genes

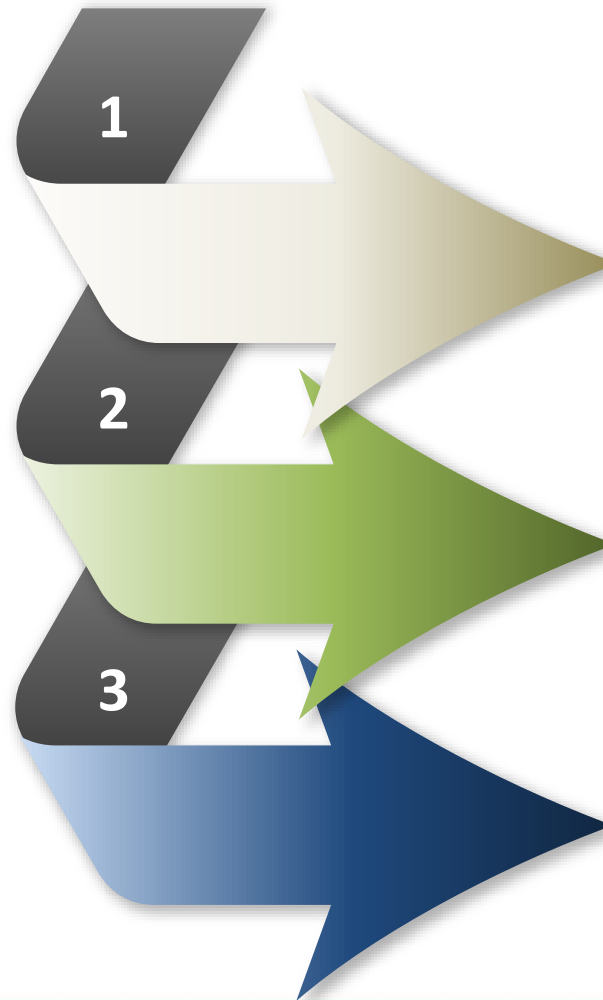
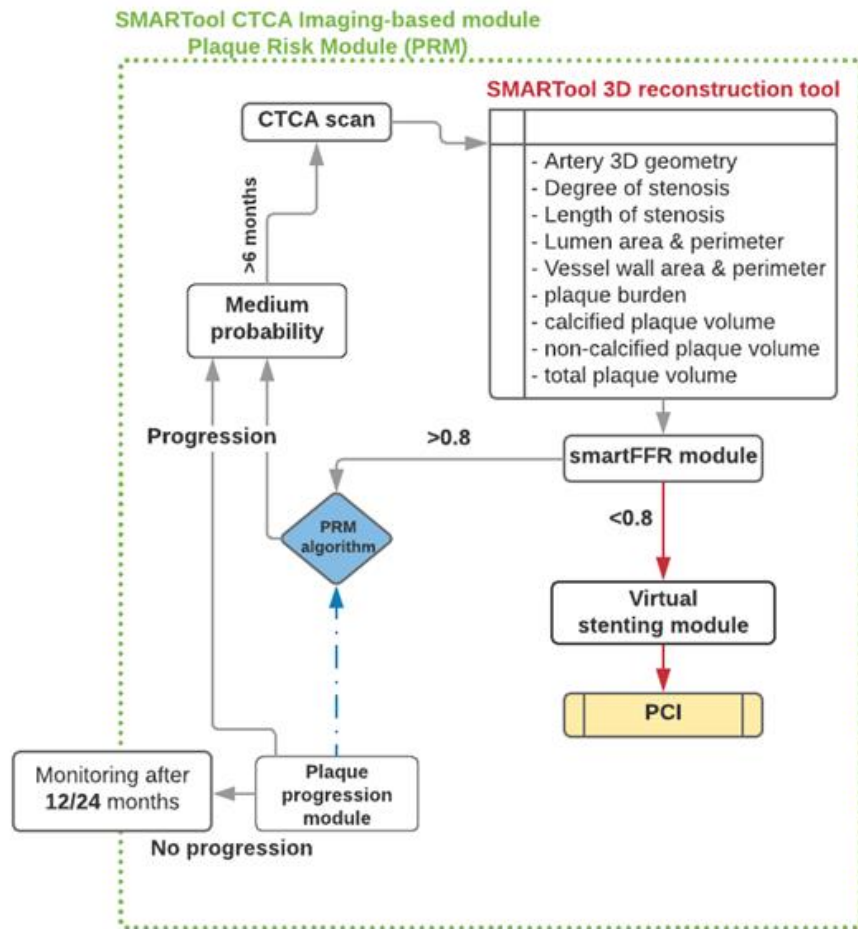
Contribution in component I



Contribution in component II



# SMARTool plaque risk module (PRM)



3D reconstruction of coronary arteries and plaque  
Several metrics will be automatically calculated and used for the estimation of plaque risk.

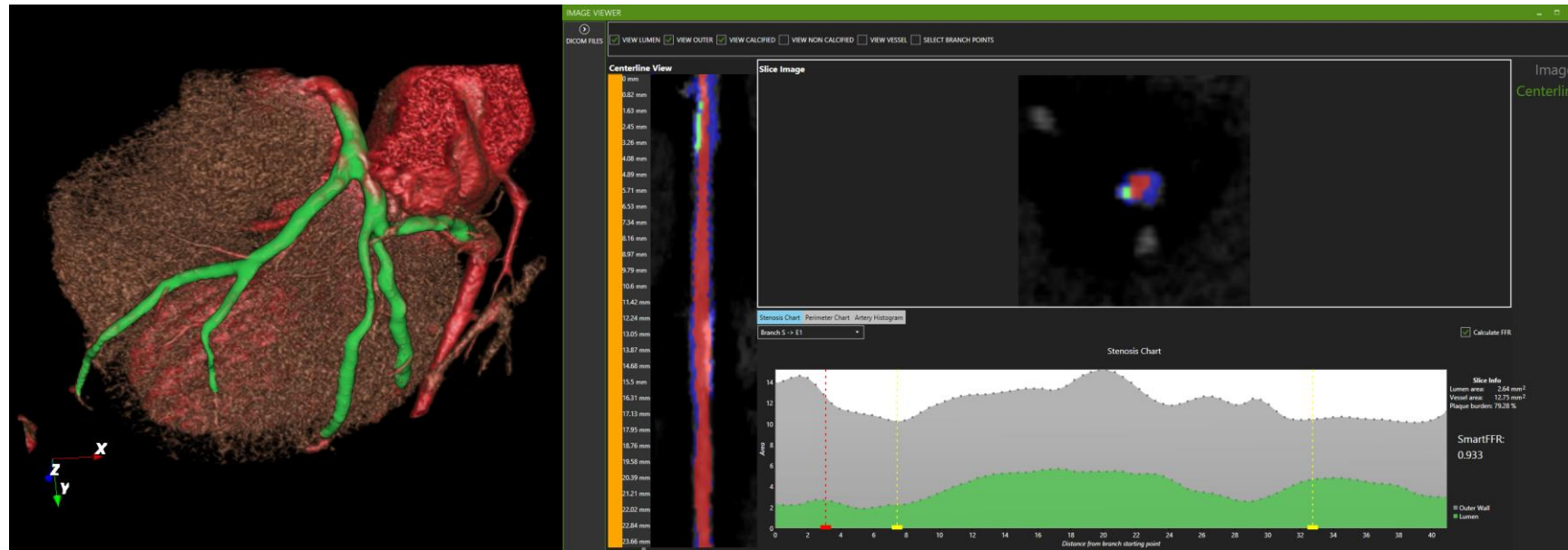
SmartFFR calculation  
Diagnosis of severity will be estimated using also the non-invasive SmartFFR calculation

Virtual stenting  
Treatment decision support is provided through a virtual stenting application



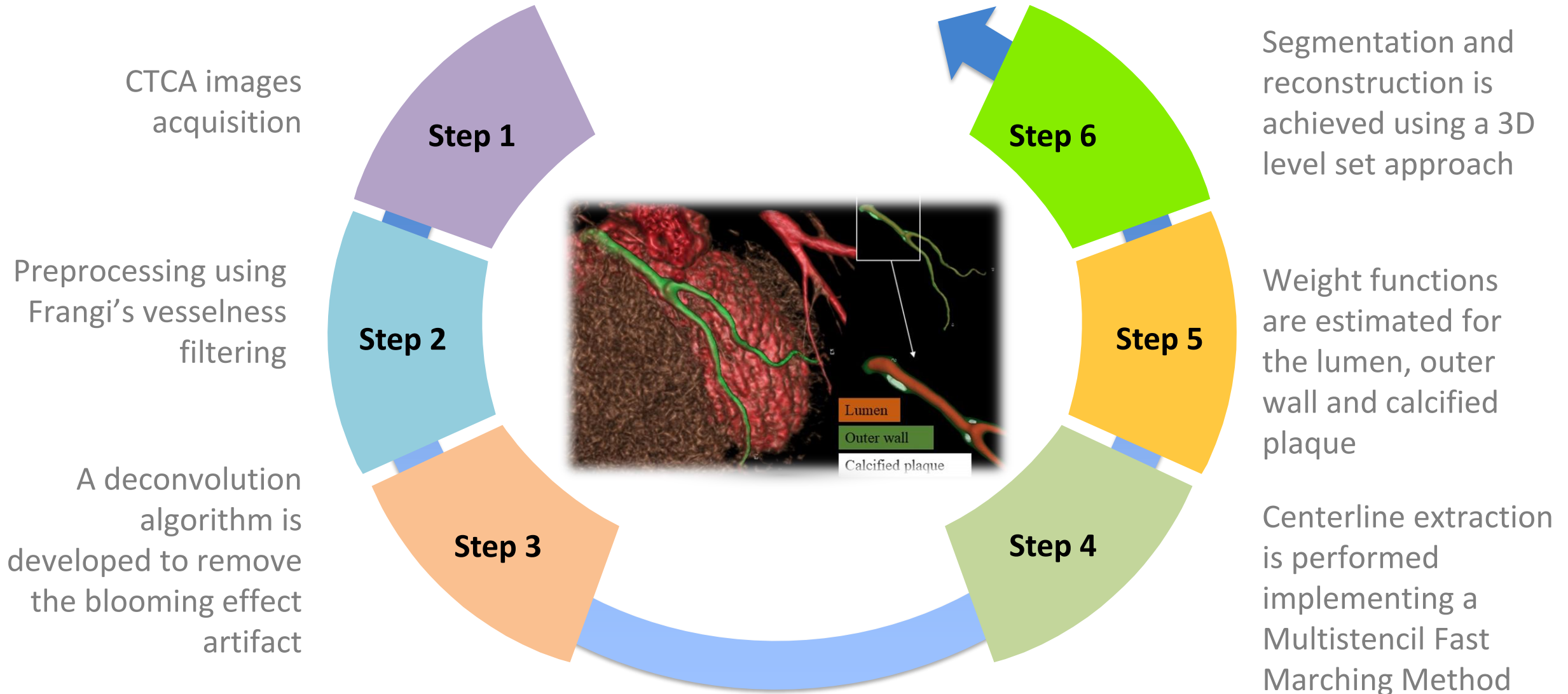
# 3D Reconstruction and plaque characterisation tool

**Aim:** to provide a user friendly semi-automate tool for the 3D reconstruction of coronary arteries, calcified and non-calcified plaques



- Several metrics are provided: Length, Lumen area and perimeter, Outer wall area and perimeter, Plaque burden, calcified plaque area and volume, Non-calcified plaque area and volume
- The metrics are provided per segment, but also for each 2D slice

# 3D Reconstruction and plaque characterisation tool



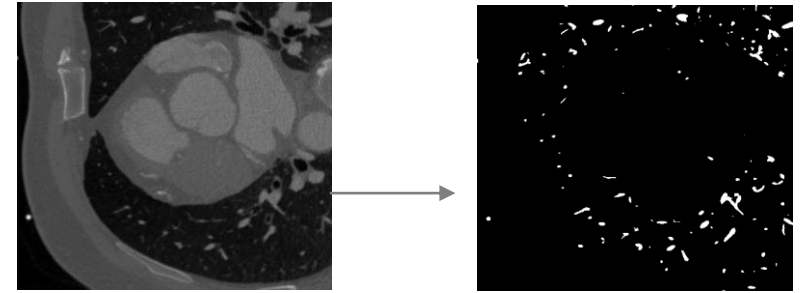
<sup>1</sup> V. I. Kigka et al., *Biomedical Signal Processing and Control*, 2018

<sup>2</sup> V. I. Kigka et al., *World Congress on Medical Physics and Biomedical Engineering*, 2018

# Pre-processing and blooming effect removal

## Preprocessing

- Contrast enhancement & image thresholding, which allows the identification of the vessel
- Implementation of Frangi Vesselness<sup>1,2</sup> filter, which permits detection of structures which correspond to coronary vessels



## Blooming effect removal

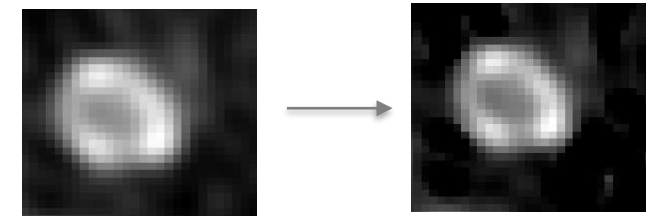
Approximation of system's PSF using a Gaussian kernel

Implementation of Deconvolution by Richardson Lucy Algorithm on high intensity regions

Improvement of the visualization of small high-density objects and blooming effect limitation

The output image of a CT system ( $f(x,y)$ ) can be modeled as the convolution of the input ( $g(x,y)$ ) with the system's PSF ( $h(x,y)$ )<sup>3</sup>

$$f(x,y) = h(x,y) * g(x,y)$$



CTA output image

Deblurred image

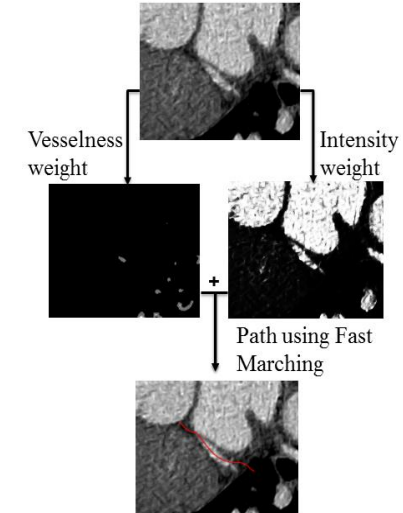
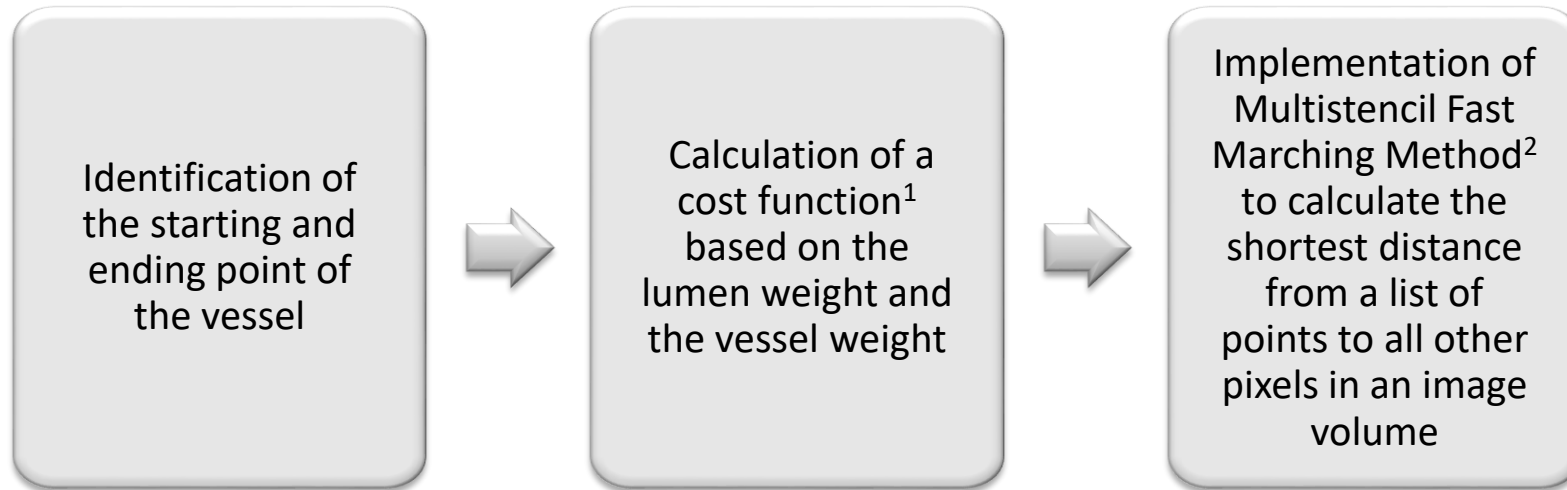
<sup>1</sup>Manniesing R., Information Processing in Medical Imaging: 19th International Conference, 2005.

<sup>2</sup>Frangi RF, Lecture Notes in Computer Science. Springer-Verlag, 1988.

<sup>3</sup>A. Castillo, SPIE, 2015.

# Centerline extraction and weight function estimation

## Centerline Extraction



## Weight function estimation

- Calculation of membership functions that are all adapted to the mean vessel intensity across the centerline, assuming that this corresponds to the mean lumen intensity.
- For the lumen a generalized bell-shaped membership function is used and for the outer wall and the plaques a sigmoidal function.

<sup>1</sup>Metz C., Med Phys, 2009.

<sup>2</sup>Bærentzen J. A., Informatics and Mathematical Modelling, DTU, 2001.

# Segmentation

## Lumen Segmentation

- Implementation of an extension of the active contour models<sup>1</sup>
- Implementation of a level set segmentation approach that incorporates a prior shape<sup>2</sup>, aiming to segment an object whose shape is similar to the given prior shape

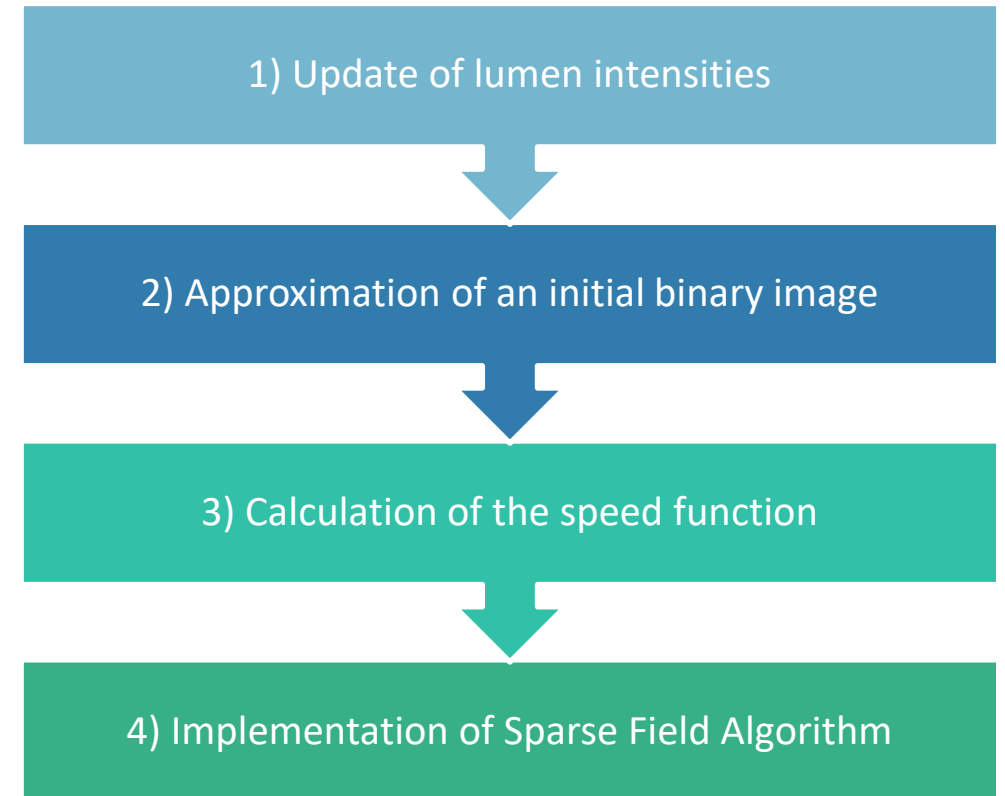
## Outer Wall Segmentation

- For the **outer wall**, the same level set approach is implemented as for the lumen segmentation.

## Plaques Segmentation

- For the **calcified plaques**, the level set is applied in the ROI of the wall.
- For the **non-calcified plaques**, a dynamic threshold-based technique is applied in the ROI of the wall.

### Segmentation approach



<sup>1</sup>Chan T.F., IEEE Transactions on image processing, 2001.

<sup>2</sup>Chan, T. F., (CVPR'05). 2005.

<sup>3</sup>Cremers D., International Conference on Scale-Space Theories in Computer Vision, 2003.

<sup>4</sup>Chan, T. F., (CVPR'05). 2005. IEEE.

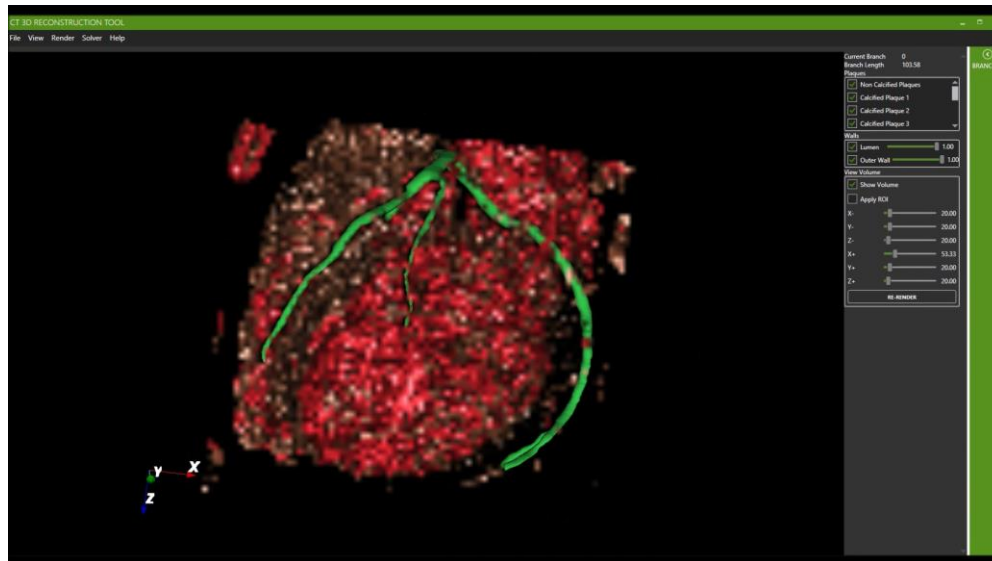
<sup>5</sup>Whitaker R.T., International journal of computer vision, 1998



# 3D geometric models reconstruction

## 3D Surface construction

- Computation of an isosurface data from the different extracted  $\varphi$ .
- Implementation of Marching Cubes algorithm, proposed by Lorensen *et al.*<sup>1</sup> to construct 3D surfaces for the lumen, outer wall and CP plaques.



<sup>1</sup>Lorensen W. E., *ACM siggraph computer graphics*, 1987.

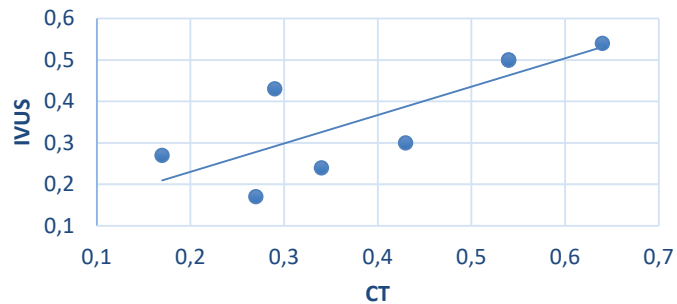


# Validation results

## Validation using **IVUS** modality

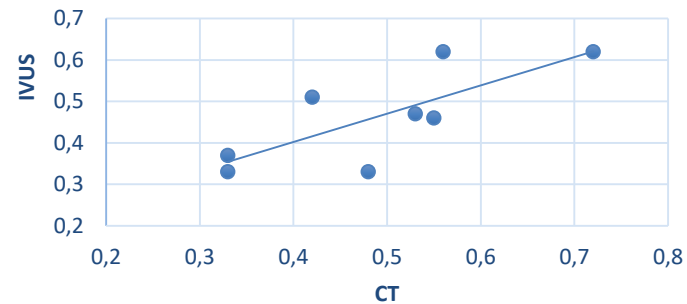
Degree of stenosis 1

( $r=0.79$ ,  $p=0.02$ )



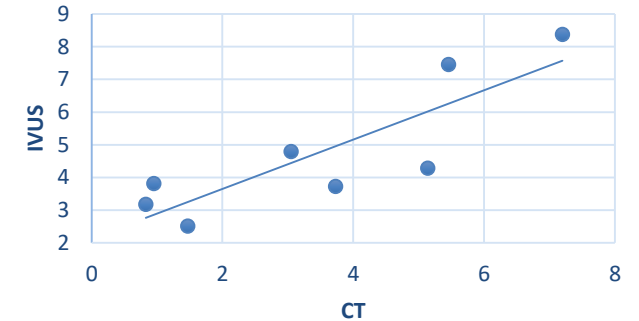
Degree of Stenosis 2

( $r=0.76$ ,  $p=0.02$ )



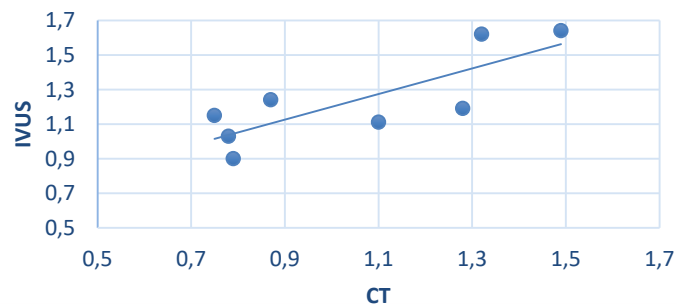
Minimal Lumen Area

( $r=0.85$ ,  $p=0.007$ )



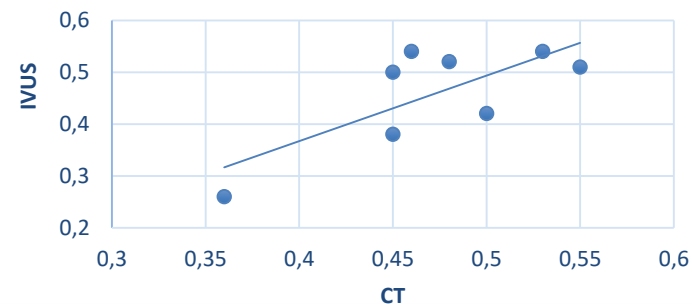
Minimal Lumen Diameter

( $r=0.81$ ,  $p=0.01$ )



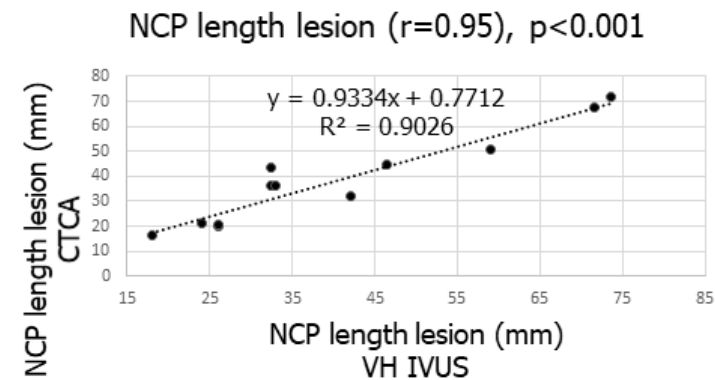
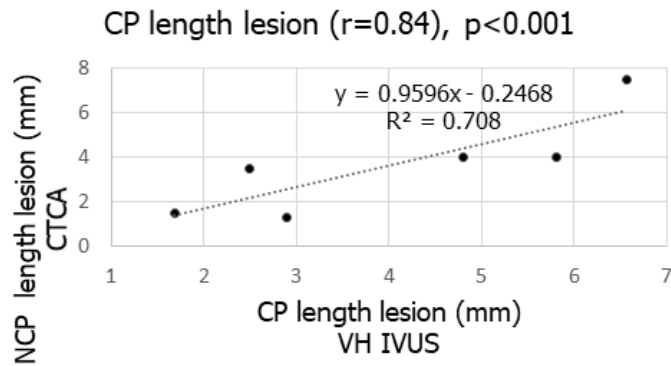
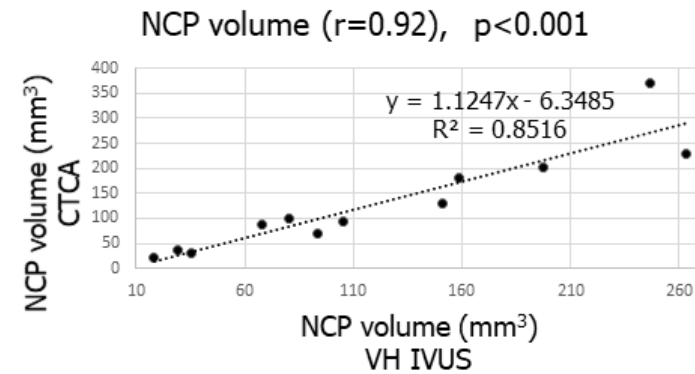
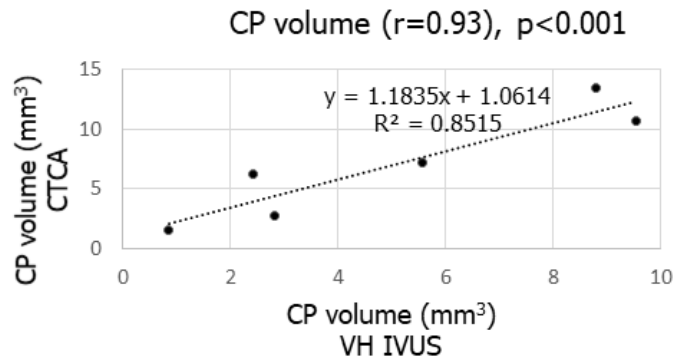
Plaque Burden

( $r=0.75$ ,  $p=0.03$ )

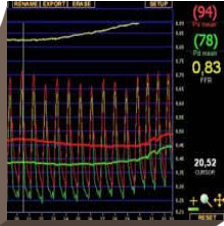


# Validation results

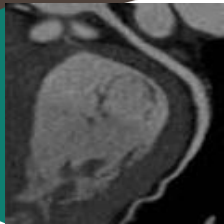
## Validation using **VH-IVUS** modality- Plaque Characterization



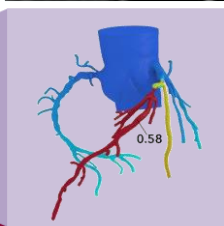
# FFR - Background



**Fractional Flow Reserve (FFR)** obtained by Invasive Coronary Angiography (ICA) is an established index for assessing the **functional significance** of a coronary lesion and making decisions for **coronary revascularization**



**Coronary computed tomography angiography (CCTA)** is the reference standard for non-invasive evaluation of the coronary anatomy



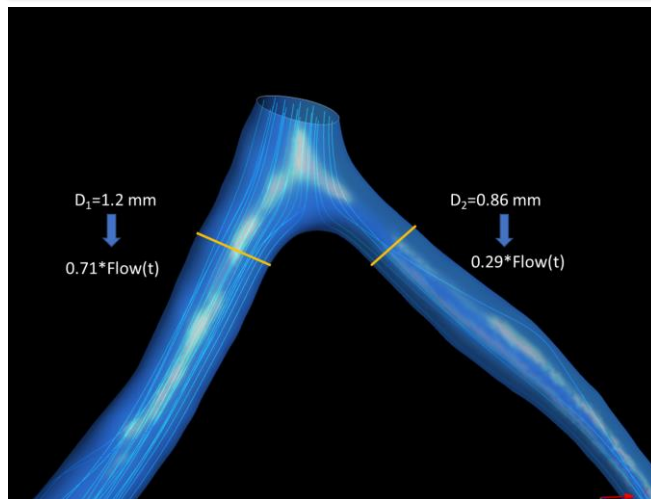
More recently, interrogation of functional significance of coronary lesions detected by CCTA has also become feasible through computation of CT-derived fractional flow reserve (**FFR<sub>CT</sub>**)



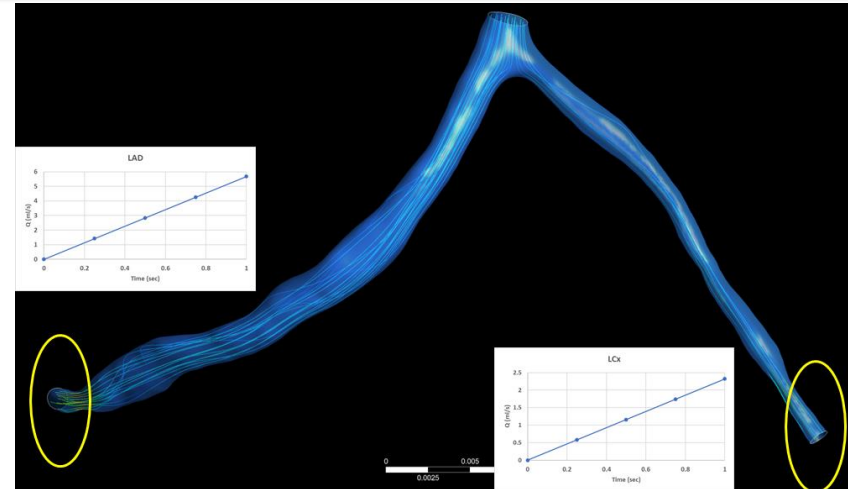
The main **drawbacks** of the CCTA-based FFR (FFR<sub>CT</sub>) methods are their **computational lengthiness** and their **need for remote core-laboratory analysis**

# SmartFFR calculation

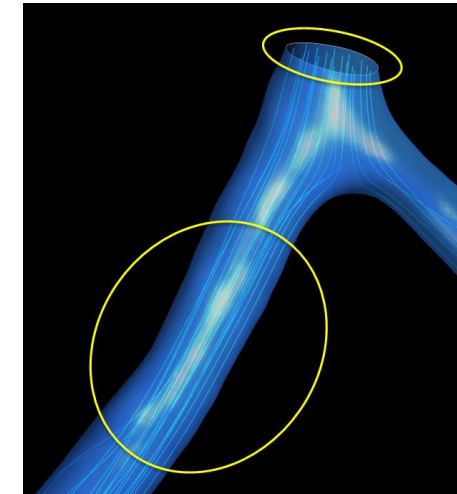
The first step is to define the necessary boundary conditions for the calculation



We apply Murray's law for the bifurcation to determine how the flow is divided for the two branches



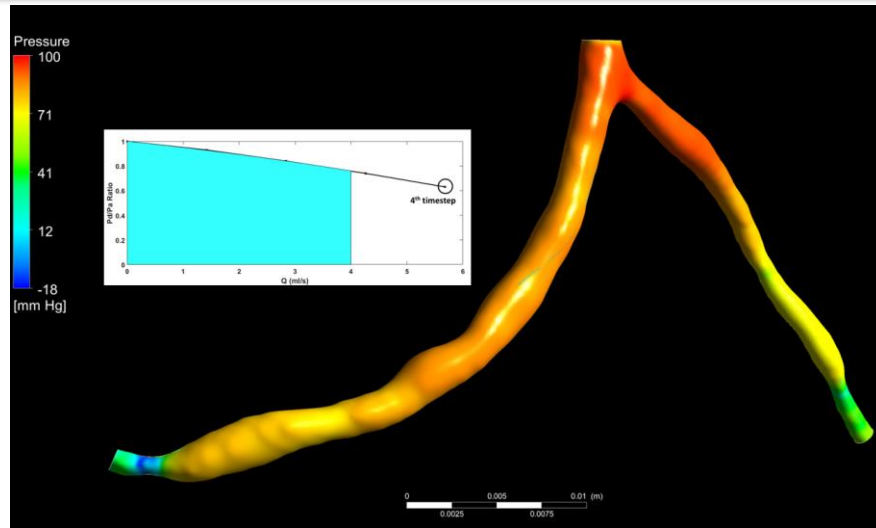
For the outlets, we perform a transient blood flow simulation assuming a developing laminar flow that begins from 0 ml/s and reaches a maximum of 8 ml/s for a total time of 1 sec divided into timesteps of 0.25 sec



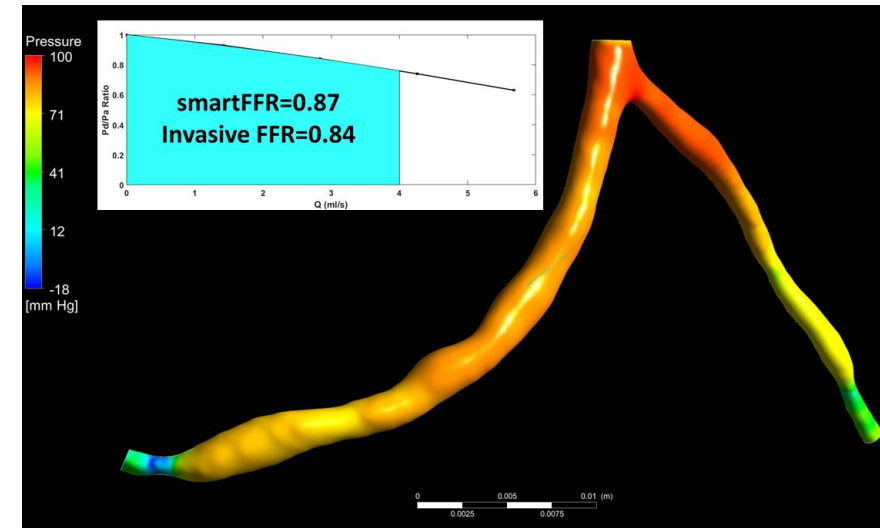
Regarding the inlet, a universal average aortic pressure value of 100 mmHg is applied

# SmartFFR calculation

The second step is to calculate the SmartFFR



We construct the patient-specific Pd/Pa curve in order to calculate the final smartFFR value



SmartFFR is computed by calculating the AUC of the Pd/Pa curve of each branch for a maximum universal flow of 4 ml/s and normalizing it to the respective AUC of the ideal healthy artery

# SmartFFR enhancements over vFAI

1

SmartFFR uses a transient increasing laminar flow simulation

2

SmartFFR uses only CFD (Pd/Pa calculated in each timestep) in order to construct the Pd/Pa vs. flow curve by connecting the calculated values through a smoothed-spline

3

The AUC is calculated through trapezoidal numerical integration of the curve

4

SmartFFR is calculated in bifurcating arteries using Murray's law to divide flow and apply the calculated values as outlet boundary conditions

5

It is faster and can be applied on more than two branches simultaneously

6

As an inlet, the patient-specific average aortic pressure will be applied

vFAI uses two separate steady state blood flow simulations

1

It simulates a flow during rest and under stress

2

vFAI uses the theoretical generalized equation to construct the Pd/Pa vs. flow curve

3

$$\Delta P = 0 + f_v Q + f_s Q^2$$

It is then calculated by integrating the aforementioned equation in its final form

4

vFAI is only applicable on segments

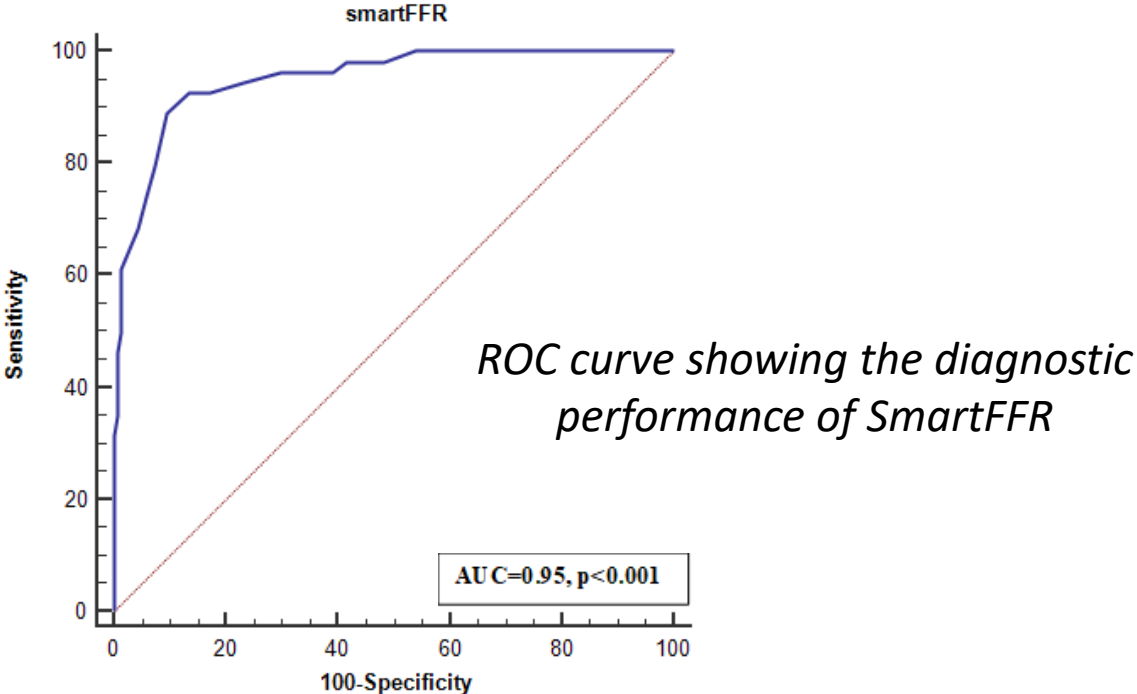
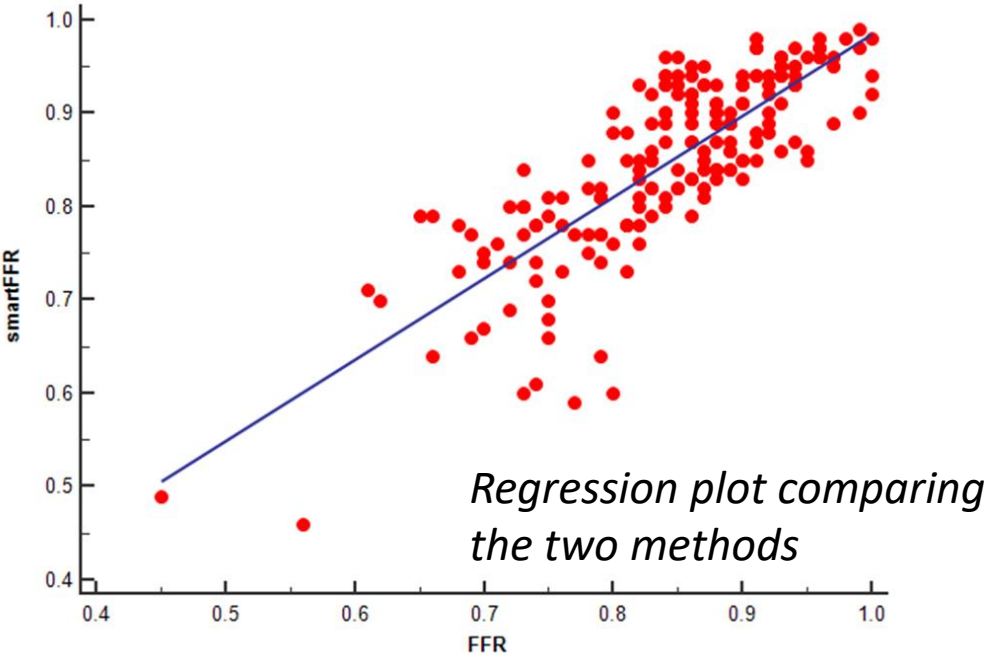
5



# Validation

- For the **validation** of the SmartFFR, we used **189 vessels of 161 patients**
- Standard per-protocol techniques were used for the ICA acquisition with multiple projections. FFR was invasively measured after the intravenous administration of 140 µg/kg/min of adenosine
- 54 vessels (28.1%) presented with a pathologic FFR value (i.e.  $\leq 0.80$ )
- From the 189 vessels, 111 were Left Anterior Descending arteries (LAD), 53 were Right Coronary Arteries (RCA) and 25 were Left Circumflex (LCx)

# Validation



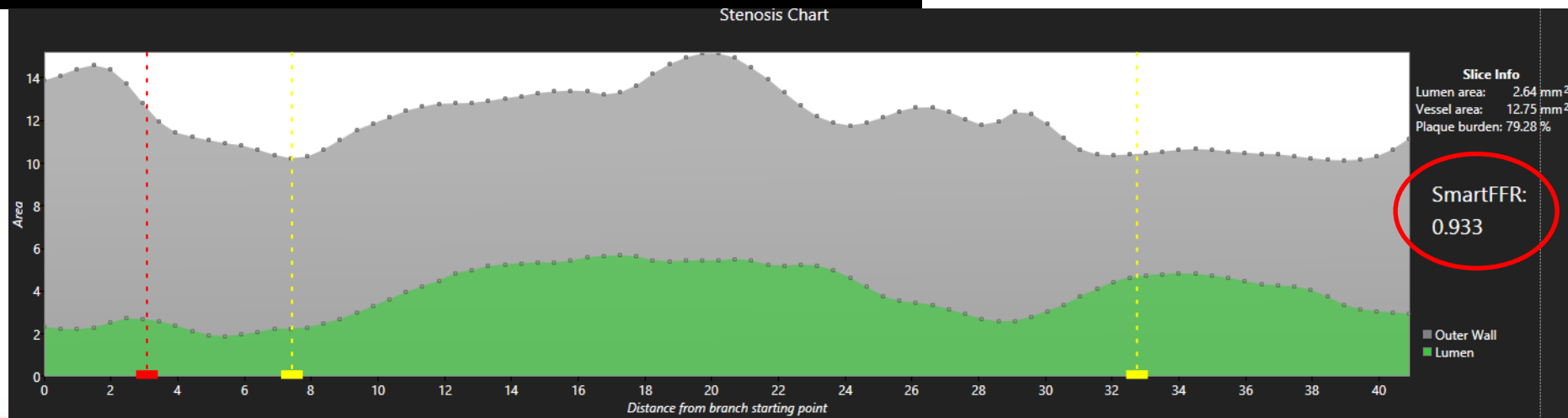
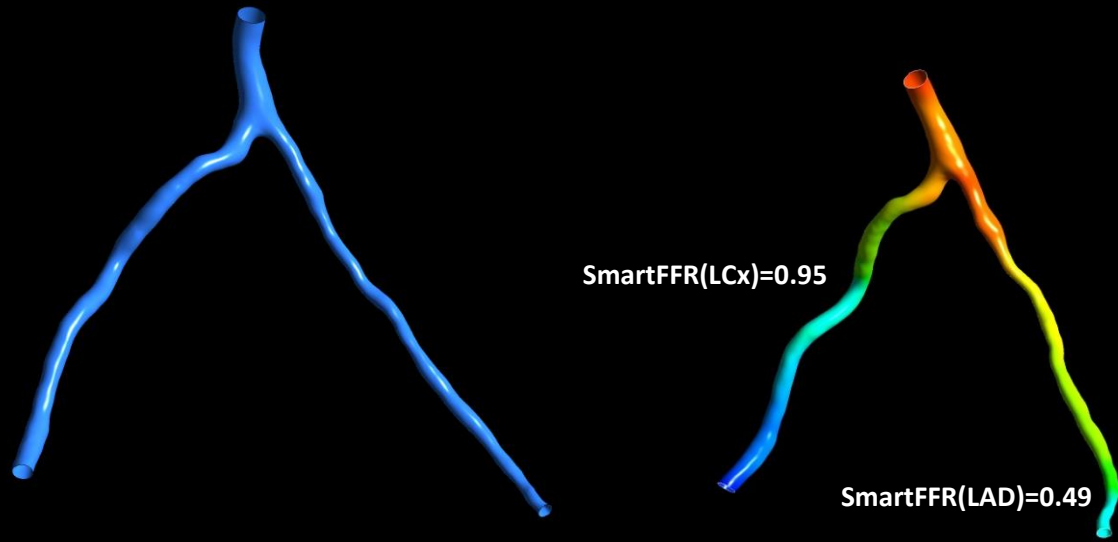
**Diagnostic performance of SmartFFR**

FFR ≤ 0.80									
	Accuracy (%)	Sensitivity (%)	Specificity (%)	PPV (%)	NPV (%)	TP	TN	FP	FN
smartFFR ≤ 0.82	88.9	92.6	87.4	74.6	96.7	50	118	17	4



# SmartFFR conclusions

- The SmartFFR is provided for the whole reconstructed artery
- It is also provided in relation to the arterial stenosis by just selecting the region of interest (two yellow dashed lines below)
- High correlation and accuracy is observed for SmartFFR compared to non-invasive FFR measurements (accuracy=88.9)



# Prediction of plaque progression and prognosis of CAD

## CCTA and prediction

Morphological characteristics depicted at CCTA of 3,158 patients were independent predictors of ACS during a mean follow-up of 3.9 years

## FFR and prediction or diagnosis

Invasive FFR or even CCTA-based virtual FFR increases the predictability accuracy for diagnostic purposes

## IBIS-4 – ESS sub-study

The accuracy of ESS and the IVUS-derived plaque characteristics in predicting disease progression has area under the curve: 0.829



## PREDICTION study

Low ESS was independently associated with disease progression  
Large plaque burden and low ESS predicted with 41% accuracy worsening lumen obstruction requiring PCI

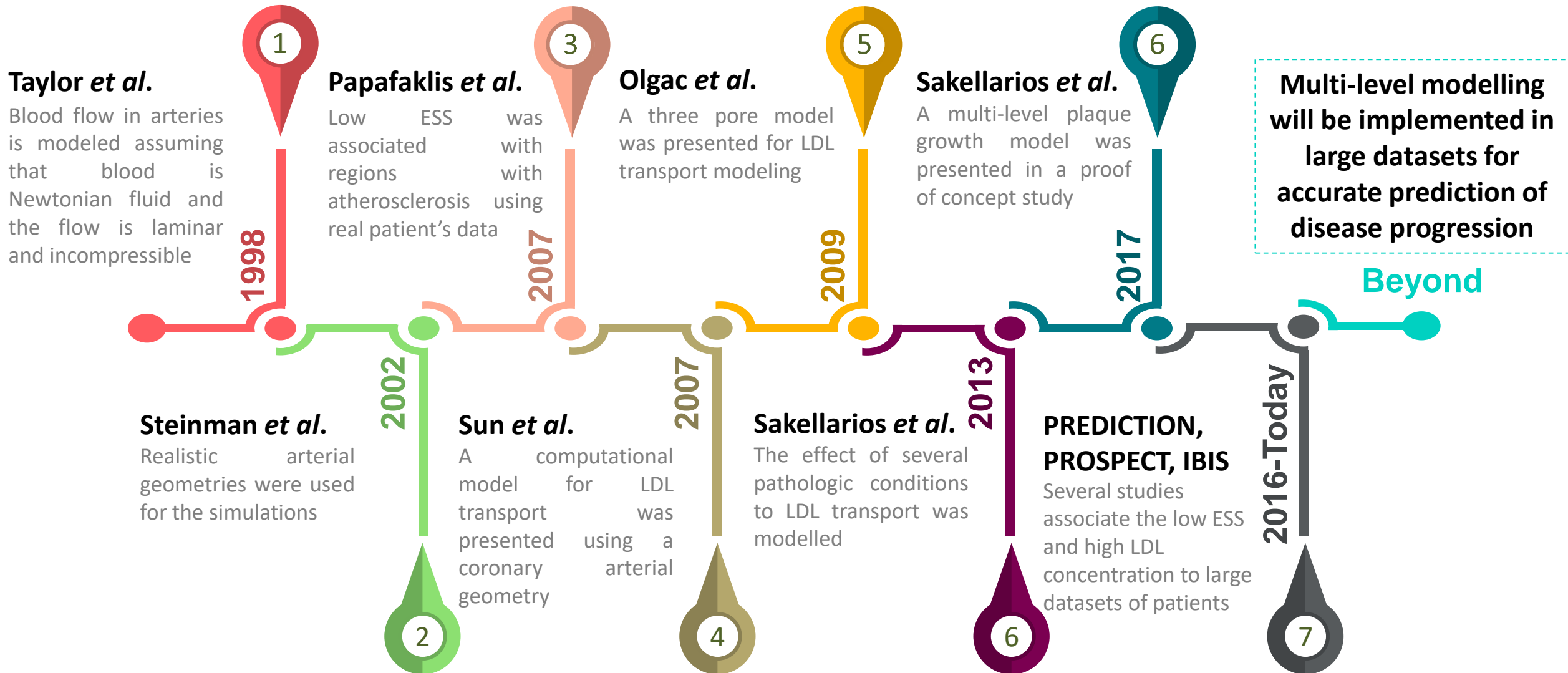
## PROSPECT study

Local low ESS provides incremental risk stratification of untreated coronary lesions in high-risk patients

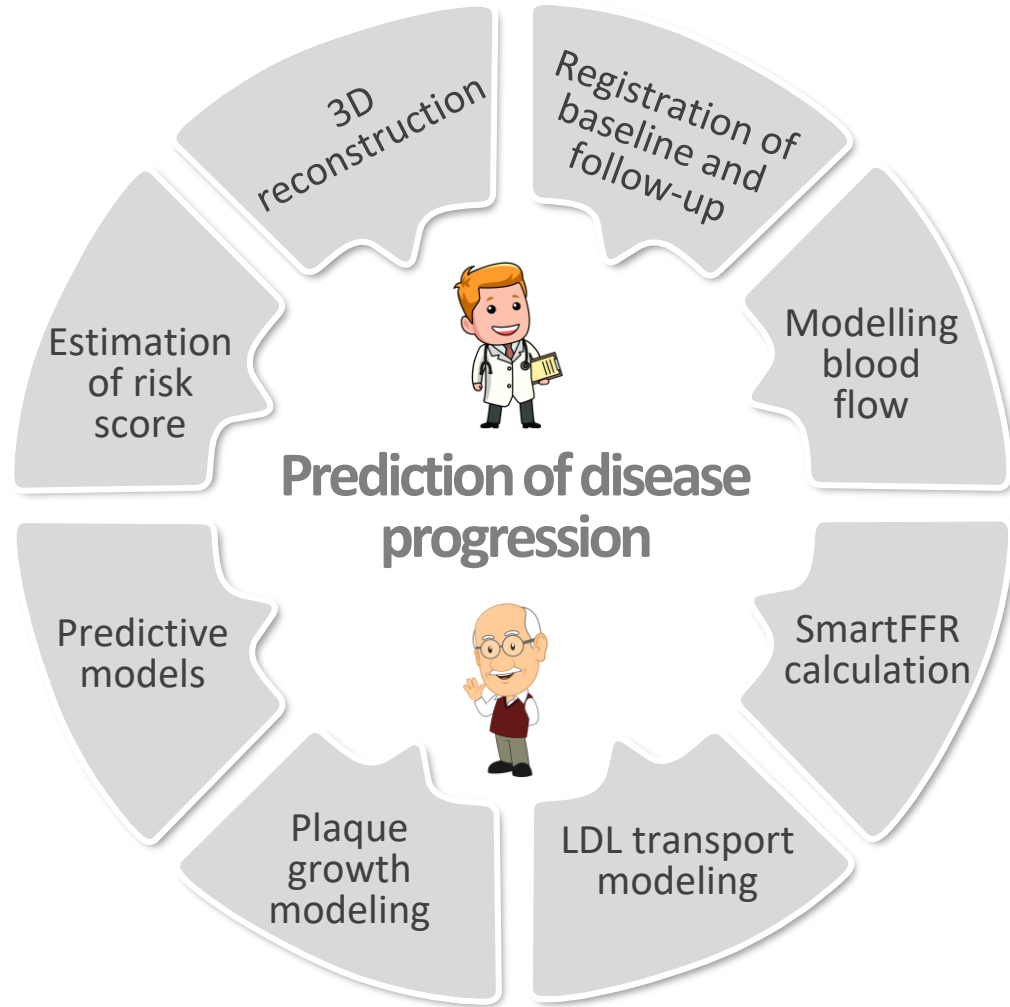
## PROSPECT-CT

The accuracy of the model of disease progression created from the predictors: Low ESS, plaque and burden, fibrofatty tissue component and fibrotic tissue was 59.0%.

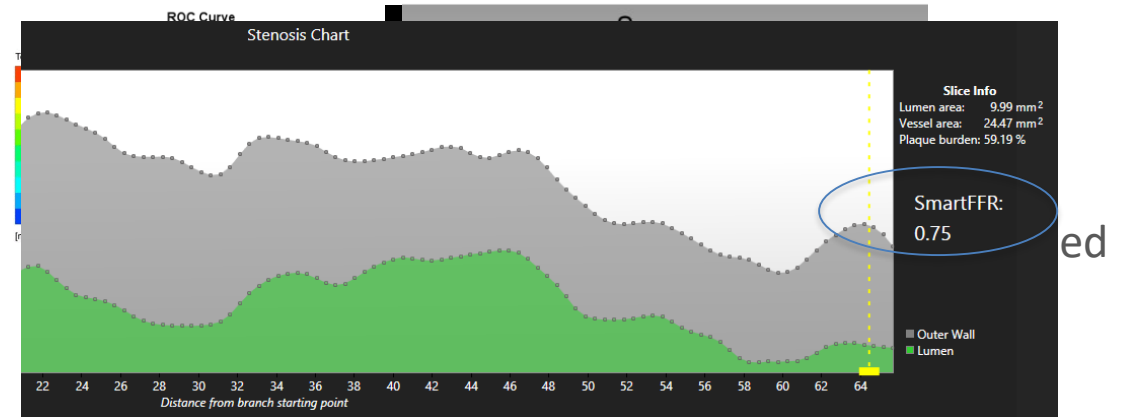
# State of the Art



# Methodological approach



## Step 4

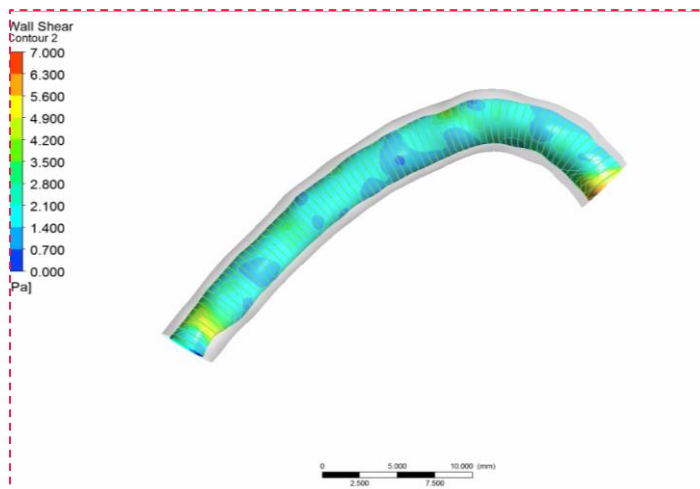


## Development of predictive models

- i) SmartFFR point model highlighting points in arteries
- ii) Machine learning models are developed



# Predictive models based on regression analysis

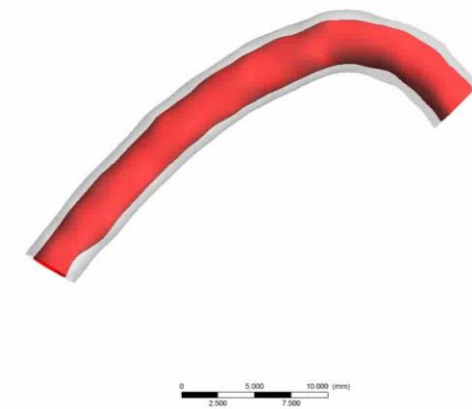


STEP 1

Computational modeling is performed at the baseline reconstructed arteries

STEP 2

Baseline and follow-up models are divided to 0.5 mm and the morphological and computational features are then extracted by 3mm



The following assumptions are made:

- The variables of lumen area, plaque area and plaque burden are transformed to binary using their median
- The progression of disease is defined as 15% lumen area reduction or 25% plaque area increase or 25% plaque burden increase

Risk score is estimated using the odds ratio from a binary logistic analysis

STEP 4

Linear regression analysis is performed to identify potential correlations

STEP 3

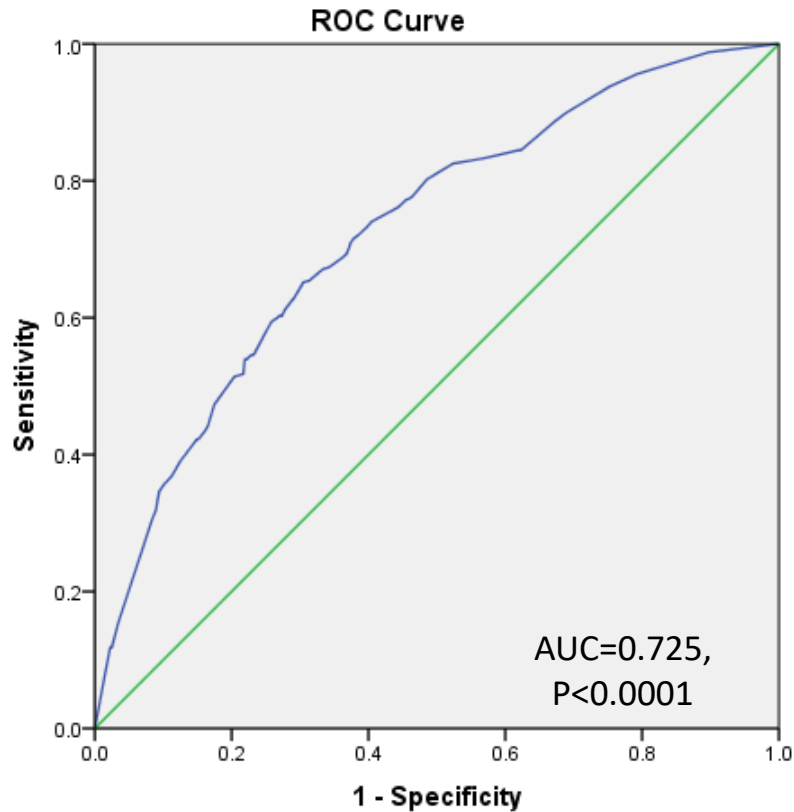
The statistical models include the following features:

- Risk factors
- Serum LDL, HDL, cholesterol, triglycerides
- Lumen area, plaque area, plaque burden
- ESS, LDL accumulation, areas of low ESS (<1.5 Pa)

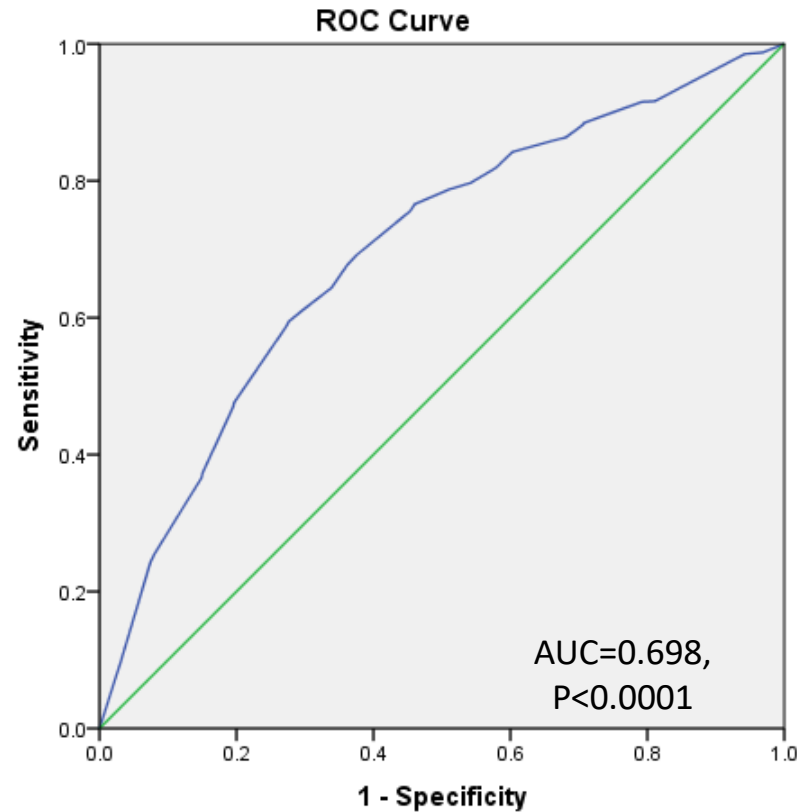
# Results

	Accuracy	Sensitivity	Specificity	PPV	NPV	Positive likelihood ratio	Negative likelihood ratio
Decreased lumen area at follow-up	0.795	0.772	0.821	0.826	0.766	0.941	0.277
Increased plaque area at follow-up	0.691	0.663	0.725	0.747	0.638	0.914	0.464
Increased plaque burden at follow-up	0.652	0.662	0.644	0.588	0.713	1.028	0.525
Lumen area progression	0.685	0.381	0.874	0.652	0.695	0.436	0.708
Plaque area progression	0.675	0.561	0.750	0.594	0.724	0.748	0.585
Plaque burden progression	0.673	0.501	0.842	0.758	0.632	0.595	0.592

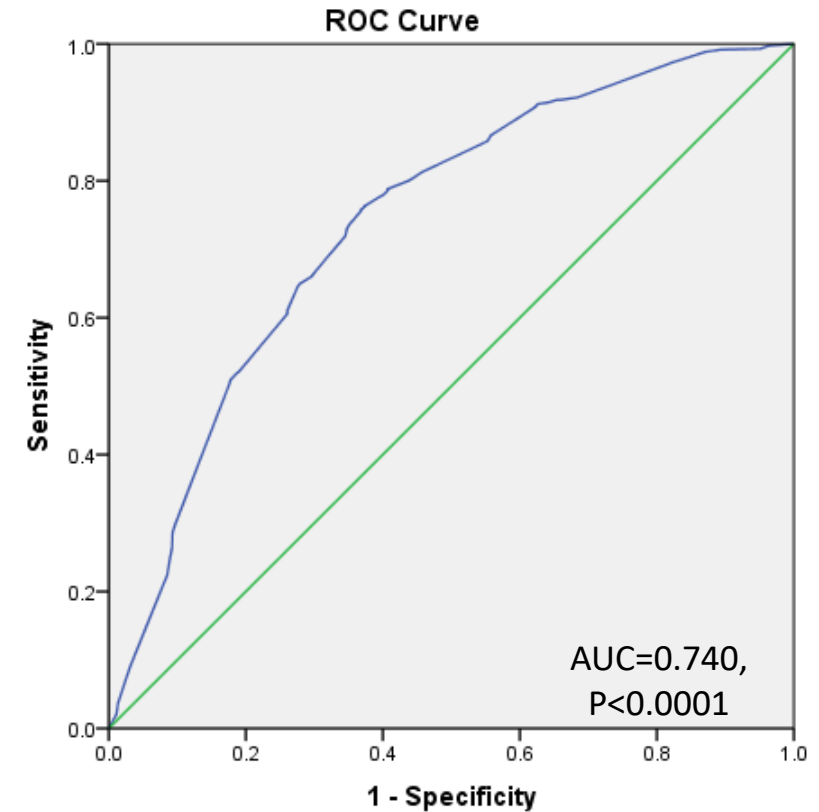
# Results



ROC curve of predictive model for lumen area decrease



ROC curve of predictive model for plaque area increase



ROC curve of predictive model for plaque burden increase

# Predictive models based on machine learning

---

CAD risk can be assessed by linear regression models of clinical, laboratory and anthropometric features, assuming linearity as well as time-invariance of the underlying input-output relationships<sup>1</sup>.

---

Clinicians attempted to predict CAD status based on established risk factors (age, total cholesterol, smoker etc.), implementing **statistical analysis** techniques.

---

In this approach, we utilize the established CAD risk factors and image based geometrical risk factors to predict CAD status in a follow-up step, using **machine learning** approaches.

<sup>1</sup>Damen, J.A., et al., *BMJ*, 2016.

<sup>2</sup>Weng, S.F., et al., *PLOS ONE*, 2017.

# State of the art

## Machine Learning Based Techniques

Exarchos *et al.*<sup>1</sup> implemented typical classification schemes (BN, NB, ANN, SVM), using demographics, clinical data, several biochemical variables, monocytes and adhesion molecules, to predict the number of vessels' stenosis, the atherosclerosis progression, as well as a hybrid score corresponding to the severity of the disease

Alizadehsani *et al.*<sup>2</sup> utilizes demographics, clinical data, echocardiography data and 54 features of laboratory variables to predict the status of CAD, applying a support vector machine (SVM) algorithm with kernel fusion.

Weng *et al.*<sup>3</sup> aimed to predict a fatal or non-fatal cardiovascular event over the ten years, using typical classification algorithms.

<sup>1</sup>Exarchos K. P., et al., *IEEE JBHI*, 2015.

<sup>2</sup>Alizadehsani R. et al., *Knowledge-Based Systems*, 2016.

<sup>3</sup>Weng, S.F., et al., *PLOS ONE*, 2017.

# State of the art

## Concept of geometrical risk factors

Atherosclerosis is non-uniformly distributed in the coronary vasculature, considering both the different human coronary arteries and the different sites of the coronary vessel<sup>1</sup>.

The conventional risk factors cannot explain this phenomenon, since their influence corresponds to the entire coronary vessel

This investigation has led to the concept of **geometric risk factors** for the evolution of atherosclerosis, having a significant influence on the mechanical environment of the coronary arterial wall<sup>2</sup>.

<sup>1</sup>Zhu H. et al., *International journal of cardiology*, 2009.

<sup>2</sup>Friedman M.H. et al., *Atherosclerosis*, 1983.



# Problem Formulation-CAD Prognosis

## Prognosis of CAD approach

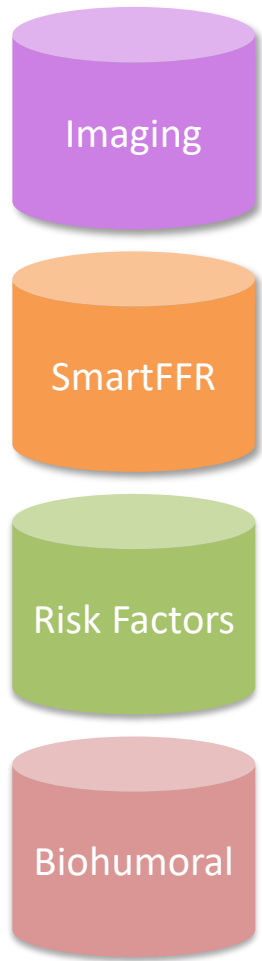
- In the presented approach, a dataset of 179 patients was used, who underwent CTCA imaging to diagnose their risk of CAD and evaluate the percentage of coronary vessels' stenosis.
- Information obtained **at time  $t$**  (baseline) is used to predict one patient's status at time  $t + h$  (follow-up), where  $h$  is the prediction horizon (in years).
- CAD risk prediction is formulated as a 2 class classification problem.
- The progression of the disease is represented as a nonlinear parametric function of a confined set of features  $f(x) = C_i, x = [x_1, \dots, x_d], i = 0, \dots, k.$

Class 0  
No CAD

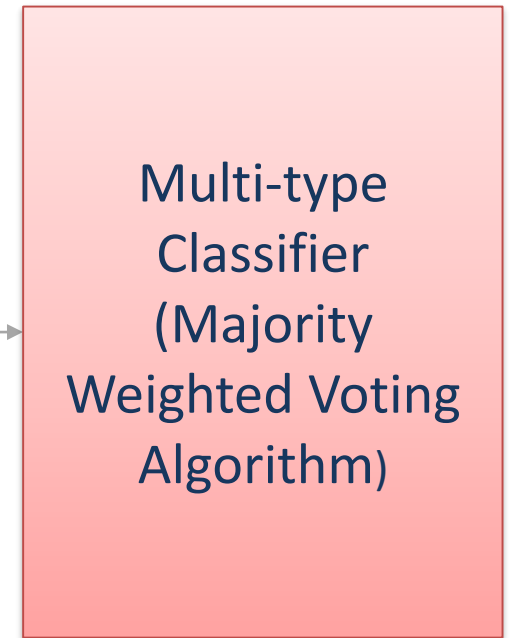
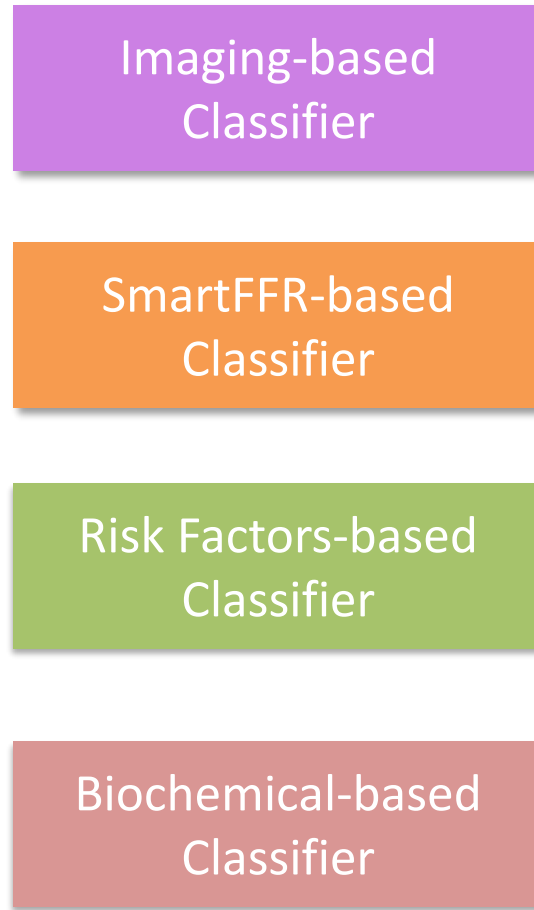
Class 1  
CAD

# Features dataset

Imaging	Risk Factors	Biochemical	
Degree of Stenosis	Age	Alanine Aminotransferase	Total Cholesterol
Minimal Lumen Area	Gender	Alkaline Phosphatase	Triglycerides
Minimal Lumen Diameter	Family History CHD	Aspartate Aminotransferase	Uric Acid
Plaque Burden	Hypertension	Creatinine	Cardiac troponin
CP Volume	Diabetes	Gamma Glutamyl Transferase	HDL total cholesterol ratio
NCP Volume	Dyslipidemia	Glucose	Statins
Count of CP	Current Smoking	HDL	ICAM1
FFR index	Past Smoking	Reactive Protein	VCAM1
	Obesity	Interleukin	
	Metabolic Syndrome	LDL	
	Current symptoms	Leptin	



# Methodology



# Results

Type of Classifier	Prediction Algorithm	Accuracy	Fusion of Classifiers
Imaging-based Classifier	Random Forest	0.79	Accuracy: <b>0.85</b>
SmartFFR-based Classifier	Support Vector Machine	0.67	
Risk Factors-based Classifier	Logistic Regression	0.68	
Biochemical-based Classifier	Random Forest	0.64	

# Problem Formulation-CAD progression

## Prediction of CAD progression

- In the presented approach, a dataset of 139 patients was used, who underwent CTCA imaging in baseline and follow-up step to diagnose their risk of CAD, evaluate their percentage of stenosis, and quantify the increase (or decrease) of atherosclerotic plaque
- Our aim is to predict the progression of atherosclerosis
- The progression of atherosclerosis is considered as the increase of plaque volume higher than 15% between the baseline and follow-up step
- Prediction of CAD progression is formulated as a 2 class classification problem.

Class 0  
No Progression

Class 1  
Progression

# Methodology

## INPUT

### Imaging

Geometrical  
Metris for each  
artery  
(LAD,LCX,RCA)  
Degree of  
Stenosis  
Minimal Lumen  
Area  
Minimal Lumen  
Diameter  
Plaque Burden  
CP Volume  
NCP Volume  
Count of CP  
FFR for each  
artery (LAD, LCX,  
RCA)

### Risk factors

Age  
Gender  
Family History  
CHD  
Hypertension  
Diabetes  
Dyslipidemia  
Current  
Smoking  
Past Smoking  
Obesity  
Metabolic  
Syndrome  
Current  
symptoms

### Biochemical

Alanine Amino-  
transferase, Alkaline,  
Phosphatase,  
Aspartate  
Aminotransferase  
Creatinine, Gamma  
Glutamyl  
Transferase  
Glucose, HDL,  
Reactive Protein,  
Interleukin, LDL,  
Leptin, Total  
Cholesterol  
Triglycerides  
Uric Acid, Cardiac  
troponin,  
Statins  
ICAM1, VCAM1



Preprocessing  
Feature Selection  
Ranking Techniques



Classification



Model Selection

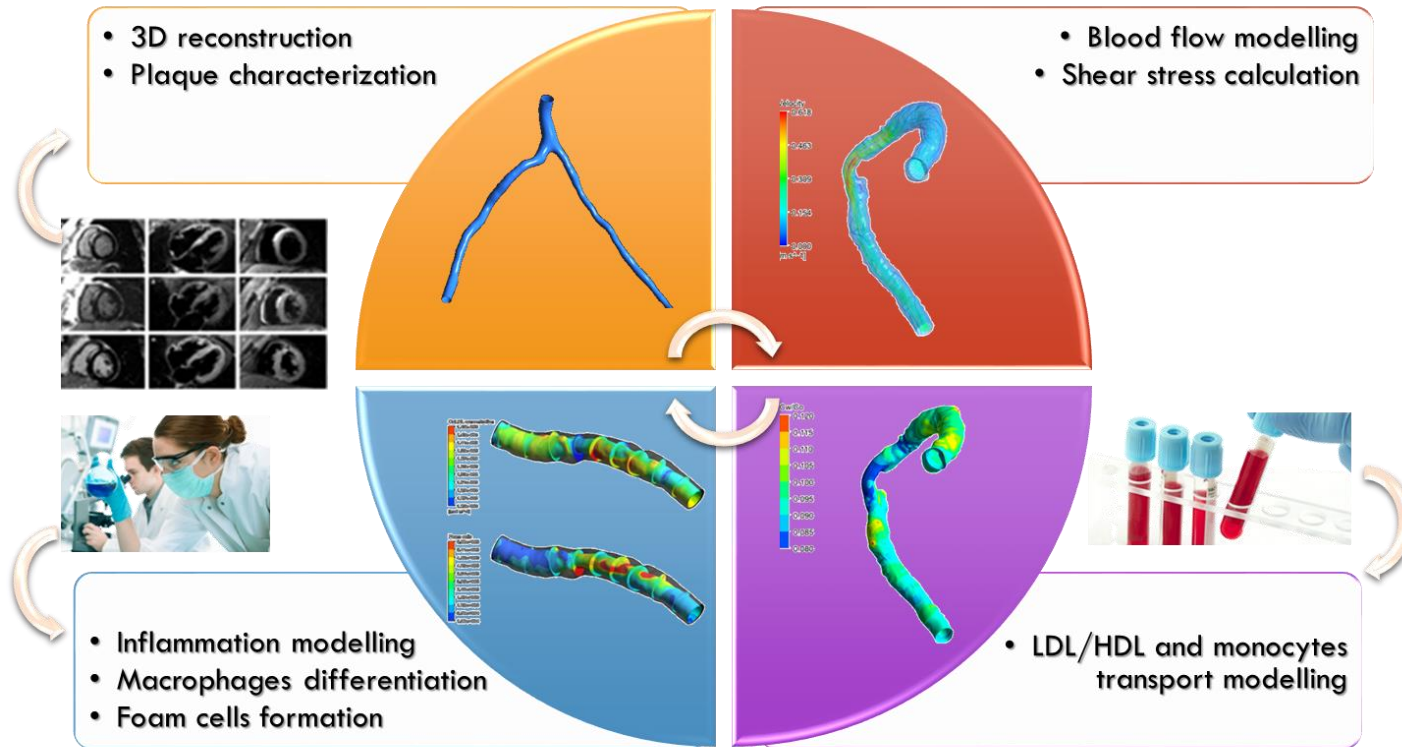




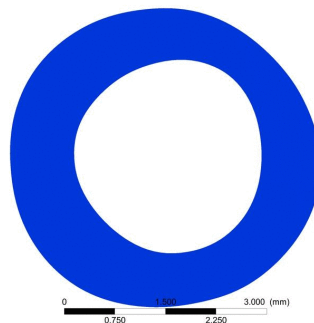
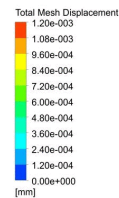
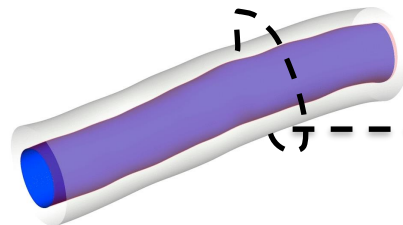
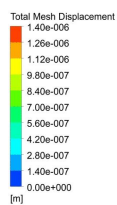
# Results

Input	Feature Selection	Prediction Algorithm	Accuracy
38 Features	Ranking Techniques (Hyperparameter optimization on the training set)	Support Vector Machine	0.63
		Logistic Regression	0.64
		Artificial Neural Networks	0.61
		Decision Trees (J48)	<b>0.67</b>

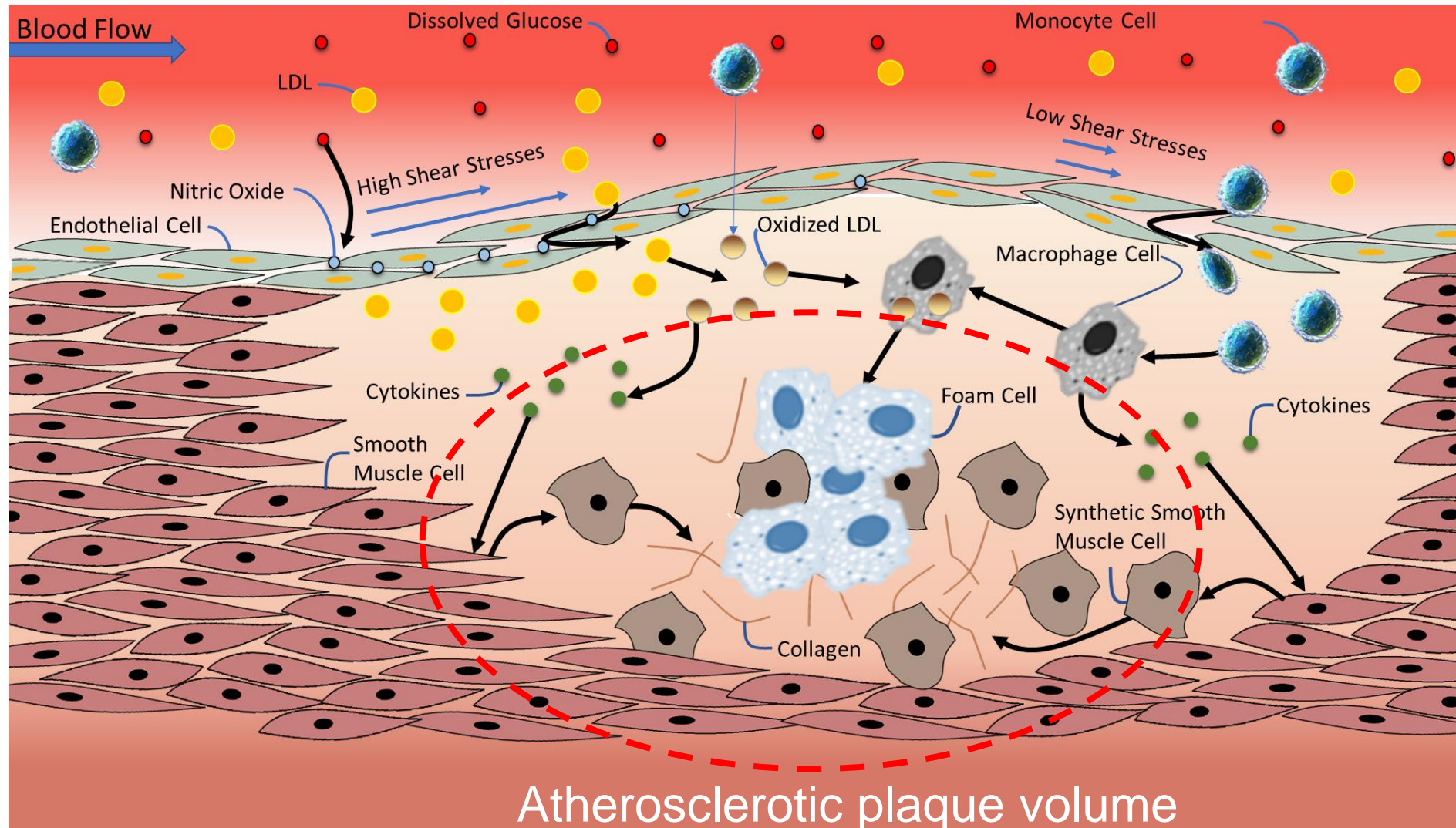
# The concept of prediction models based on plaque growth modeling in SMARTool



- A novel model for plaque growth prediction
- It combines computational modeling and machine learning in order to predict regions which are prone to disease evolution
- The concept is based on the assumption that any additional level of information will increase the prediction accuracy



# Methodological approach of plaque growth in SMARTool



# Model Assumptions

Blood is considered as an incompressible homogenous fluid.

LDL, Oxidized LDL, Monocytes, Macrophages, Foam cells, Contractile and Synthetic Smooth Muscle cells, cytokines and collagen are considered substances that does not affect blood flow.

Arterial wall is considered as a homogenous porous material.

Plasma is considered to flow into the arterial wall.

The removal of plasma into the arterial wall doesn't change the blood's density and viscosity.

Endothelium layer is considered as a thin interface, through which flow rates are regulated by the Kedem-Katchalsky equations.

The osmotic pressure across the endothelium layer is neglected.



# Model Analysis

## Blood flow & substances' concentration in the lumen

- Blood flow is modeled as in the previous model but now time changes are considered.
- LDL, HDL and monocytes/macrophages concentration equations now consider time changes as well.

$$\rho\gamma \frac{\partial c_{LDL}}{\partial t} + \frac{\partial}{\partial x_i} (\rho U_j c_{LDL}) = \rho D_{LDL,lumen} \frac{\partial}{\partial x_i} \left( \frac{\partial}{\partial x_j} c_{LDL} \right)$$

$$\rho\gamma \frac{\partial c_{HDL}}{\partial t} + \frac{\partial}{\partial x_i} (\rho U_j c_{HDL}) = \rho D_{HDL,lumen} \frac{\partial}{\partial x_i} \left( \frac{\partial}{\partial x_j} c_{HDL} \right)$$

$$\rho\gamma \frac{\partial c_m}{\partial t} + \frac{\partial}{\partial x_i} (\rho U_j c_m) = \rho D_{m,lumen} \frac{\partial}{\partial x_i} \left( \frac{\partial}{\partial x_j} c_m \right)$$

# Model Analysis

## Plasma flow & substances' concentration in the arterial wall 1/4

- Blood flow is modeled as in the previous model but now time changes are considered.
- The LDL, HDL and monocyte concentrations are calculated based on the equations [1,2]:

$$\rho\gamma \frac{\partial c_{LDL}}{\partial t} + \frac{\partial}{\partial x_i} (\rho(\mathbf{K} \cdot \mathbf{U})_j c_{LDL}) = \rho K_{lag} D_{LDL} \frac{\partial}{\partial x_i} \left( \mathbf{K} \cdot \frac{\partial}{\partial x_j} c_{LDL} \right) + r_{LDL} c_{LDL}$$

$$\rho\gamma \frac{\partial c_{HDL}}{\partial t} + \frac{\partial}{\partial x_i} (\rho(\mathbf{K} \cdot \mathbf{U})_j c_{HDL}) = \rho D_{HDL} \frac{\partial}{\partial x_i} \left( \mathbf{K} \cdot \frac{\partial}{\partial x_j} c_{HDL} \right) - HDL_{protection}$$

$$\rho\gamma \frac{\partial c_m}{\partial t} + \frac{\partial}{\partial x_i} (\rho(\mathbf{K} \cdot \mathbf{U})_j c_m) = \rho D_{m,plasma} \frac{\partial}{\partial x_i} \left( \mathbf{K} \cdot \frac{\partial}{\partial x_j} c_m \right) - \underbrace{d_m c_m}_{\substack{\text{Differentiation} \\ \text{into} \\ \text{macrophages}}} - \underbrace{m_d c_m}_{\substack{\text{Apoptosis} \\ \text{s}}}$$

- For every cell, the advection term is disregarded, due to their size that does not allow the advection movement in a porous domain.

[1] A. I. Sakellarios, et al., 2013, *Journal of Physiology-Heart and Circulatory Physiology*, vol. 304, pp. H1455-H1470, Jun 2013.

[2] M. Cilla et al, *Journal of the Royal Society Interface*, vol. 11, Jan 6 2014



# Model Analysis

## Plasma flow & substances' concentration in the arterial wall 2/4

- The Macrophage, Cytokine, Oxidized LDL concentrations are calculated based on the equations:

$$\cancel{\gamma \frac{\partial c_M}{\partial t} + \frac{\partial}{\partial x_i} (\rho(\mathbf{K} \cdot \mathbf{U})_j c_M)} = \rho D_M \frac{\partial}{\partial x_i} \left( \mathbf{K} \cdot \frac{\partial}{\partial x_j} c_M \right) + \underbrace{d_m c_m}_{\text{Differentiation from monocytes}} - \underbrace{k_1 c_{OxLDL} c_M}_{\text{Differentiation into foam cells}}$$

$$\gamma \frac{\partial c_{OxLDL}}{\partial t} + \frac{\partial}{\partial x_i} (\rho(\mathbf{K} \cdot \mathbf{U})_j c_{OxLDL}) = \rho D_{OxLDL} \frac{\partial}{\partial x_i} \left( \mathbf{K} \cdot \frac{\partial}{\partial x_j} c_{OxLDL} \right) + \underbrace{r_{LDL} c_{LDL}}_{\text{LDL oxidation}} - \underbrace{k_2 c_{OxLDL} c_M}_{\text{Uptake by macrophages}} - HDL_{\text{protection}}$$

$$\cancel{\gamma \frac{\partial c_c}{\partial t} + \frac{\partial}{\partial x_i} (\rho(\mathbf{K} \cdot \mathbf{U})_j c_c)} = \cancel{\rho D_c \frac{\partial}{\partial x_i} \left( \mathbf{K} \cdot \frac{\partial}{\partial x_j} c_c \right)} - \underbrace{d_c c_c}_{\text{Degradation}} + \underbrace{d_r c_{OxLDL} c_M}_{\text{Production from OxLDL \& macrophages}}$$

- The convection and diffusion terms of cytokine concentration are disregarded, because cytokines are considered to be retained in the macrophage membrane.

# Model Analysis

## Plasma flow & substances' concentration in the arterial wall 3/4

- The Foam and Contractile Smooth Muscle cells (SMCs) concentrations are calculated based on the equations:

$$\begin{aligned}
 \gamma \frac{\partial c_F}{\partial t} + \frac{\partial}{\partial x_i} (\rho (\mathbf{K} \cdot \mathbf{U})_j c_F) &= \rho D_F \frac{\partial}{\partial x_i} \left( \mathbf{K} \cdot \frac{\partial}{\partial x_j} c_F \right) + \frac{k_1 c_{OxLDL} c_M}{\text{Differentiation from macrophages}} \\
 \gamma \frac{\partial c_{S_c}}{\partial t} + \frac{\partial}{\partial x_i} (\rho (\mathbf{K} \cdot \mathbf{U})_j c_{S_c}) &= \rho D_{S_c} \frac{\partial}{\partial x_i} \left( \mathbf{K} \cdot \frac{\partial}{\partial x_j} c_{S_c} \right) - \frac{\left( 1 + e^{\frac{-S_r c_c}{c_{c,max}}} \right) c_{S_c}}{\text{Production of Synthetic SMCs}}
 \end{aligned}$$

- The convection and diffusion terms are disregarded due to the size of smooth muscle cells.

# Model Analysis

## Plasma flow & substances' concentration in the arterial wall 4/4

- The Synthetic Smooth Muscle cells (SMCs) and collagen concentrations are calculated based on the equations:

$$\cancel{\gamma \frac{\partial c_{S_S}}{\partial t} + \cancel{\frac{\partial}{\partial x_i} (\rho (\mathbf{K} \cdot \mathbf{U})_j c_{S_S})}} = \cancel{\rho D_{S_S} \frac{\partial}{\partial x_i} \left( \mathbf{K} \cdot \frac{\partial}{\partial x_j} c_{S_{CS}} \right)} + \underbrace{\left( 1 + e^{\frac{-S_r c_c}{c_{c,max}}} \right) c_{S_C}}_{\text{Production of Synthetic SMCs}}$$

$$\cancel{\gamma \frac{\partial c_G}{\partial t} + \cancel{\frac{\partial}{\partial x_i} (\rho (\mathbf{K} \cdot \mathbf{U})_j c_G)}} = \cancel{\rho D_G \frac{\partial}{\partial x_i} \left( \mathbf{K} \cdot \frac{\partial}{\partial x_j} c_G \right)} + \underbrace{g_r c_{S_C} - d_g c_G}_{\text{Secretion from Degradation Synthetic SMCs}}$$

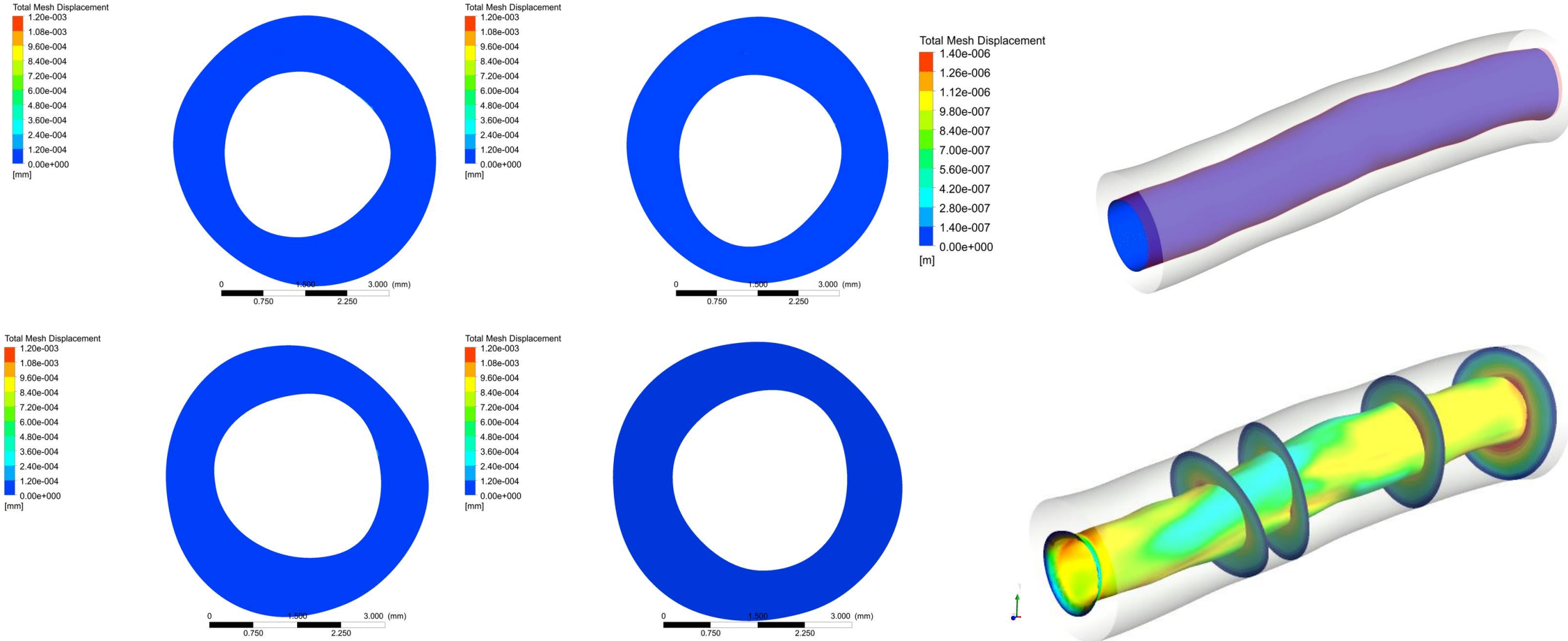
- The convection and diffusion terms are disregarded due to the size of smooth muscle cells.
- This model accounts only for the collagen secreted by the synthetic smooth muscle cells, as this is responsible for the development of atheroma plaque.
- Plaque is considered to consist of Foam cells, synthetic smooth muscle cells and collagen.

$$V_{plaque} = c_F * F\_volume + c_S * S\_volume + c_G * G\_volume$$

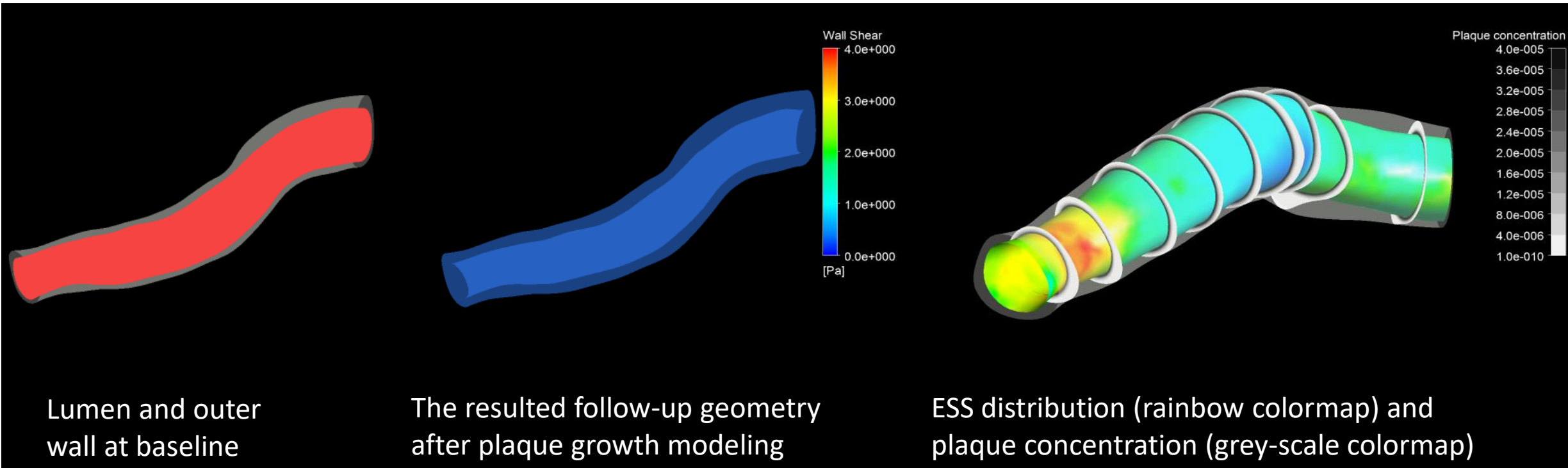
# SMARTool's plaque growth model

Model Parameters	ARTREAT model	SMARTool model
Time dependence	<i>Steady</i>	<i>Transient</i>
Substances in lumen	<i>LDL, HDL Monocytes</i>	<i>LDL, HDL Monocytes</i>
Substances in intima	<i>LDL, HDL Macrophages (Monocytes immediately differentiate to macrophages) Oxidized LDL Cytokines Foam cells</i>	<i>LDL, HDL Monocytes Macrophages Oxidized LDL (new approach) Cytokines (new approach) Foam cells (new approach) Contractile SMCs Synthetic SMCs Collagen</i>
Atherosclerotic plaque composition	<i>Foam cells</i>	<i>Foam cells Synthetic SMCs Collagen</i>
Wall thickening	<i>No</i>	<i>Yes</i>

# Results - Arterial lumen reduction

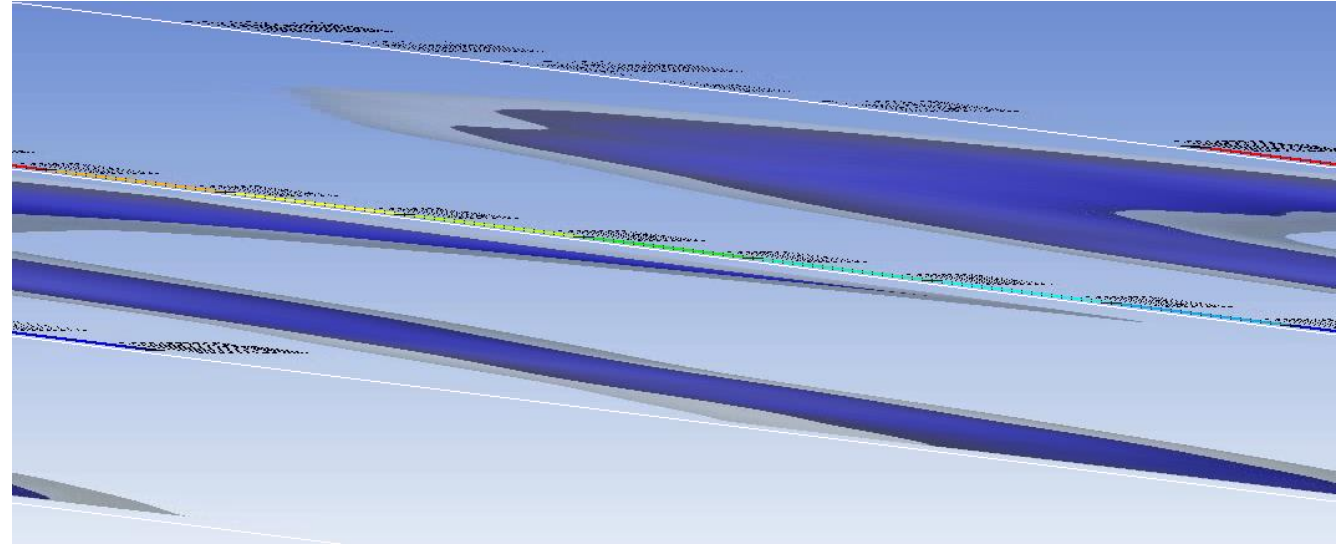
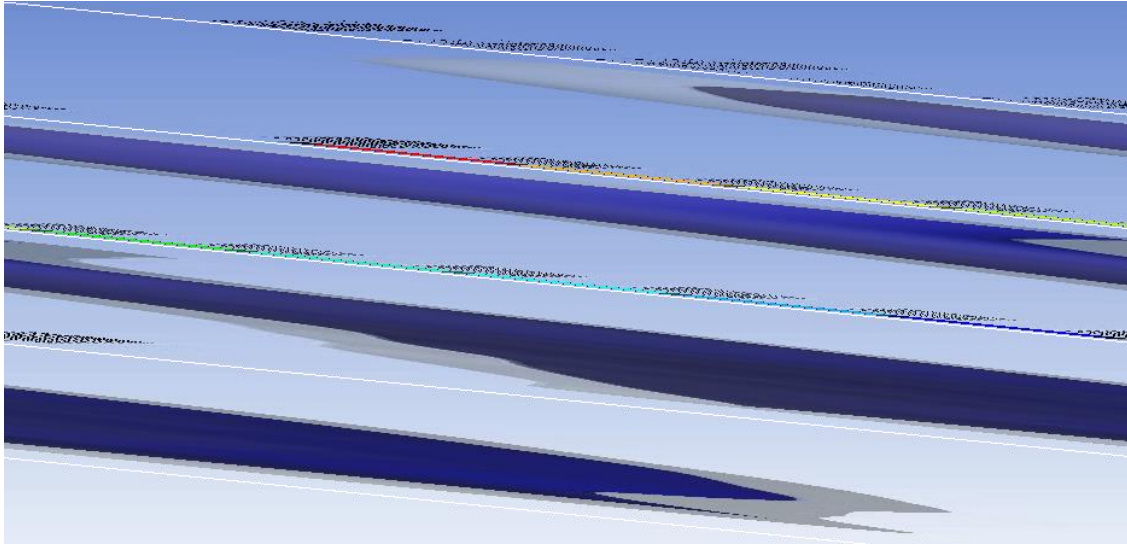


# Results

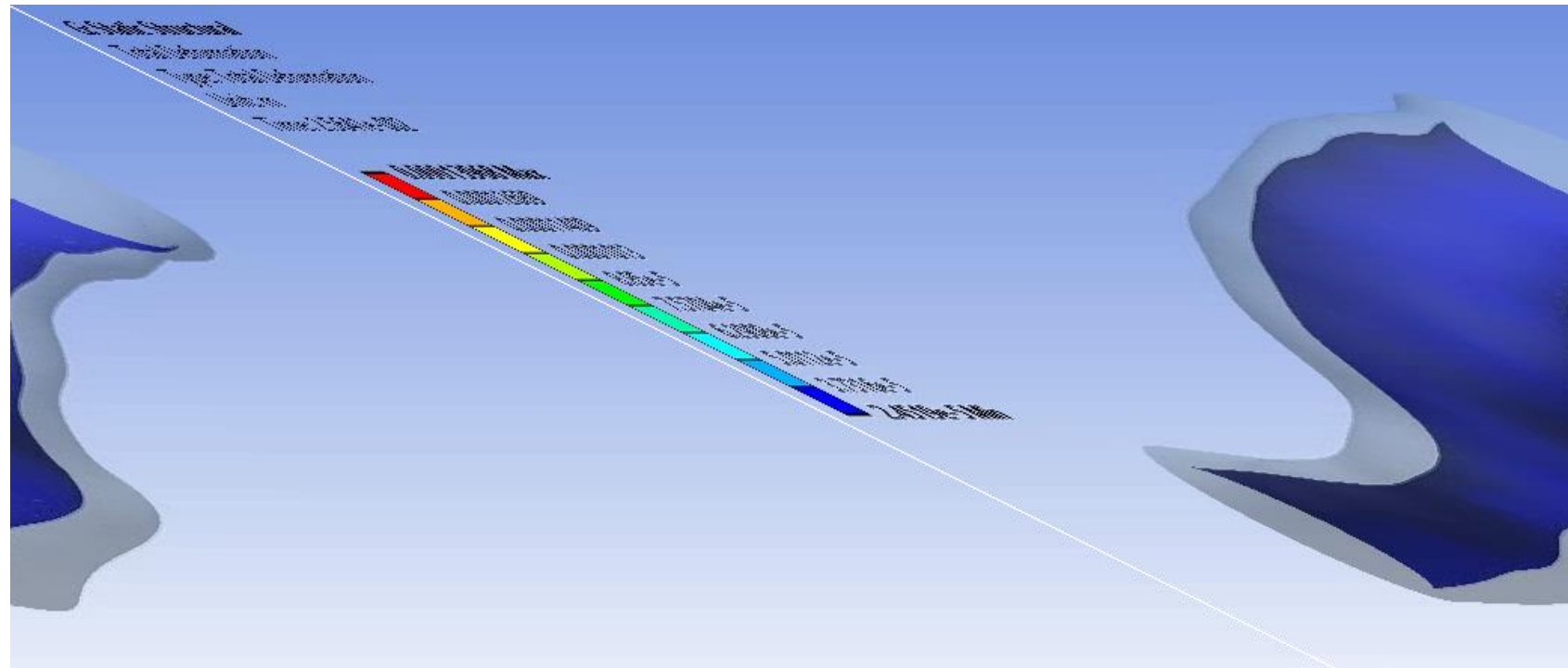
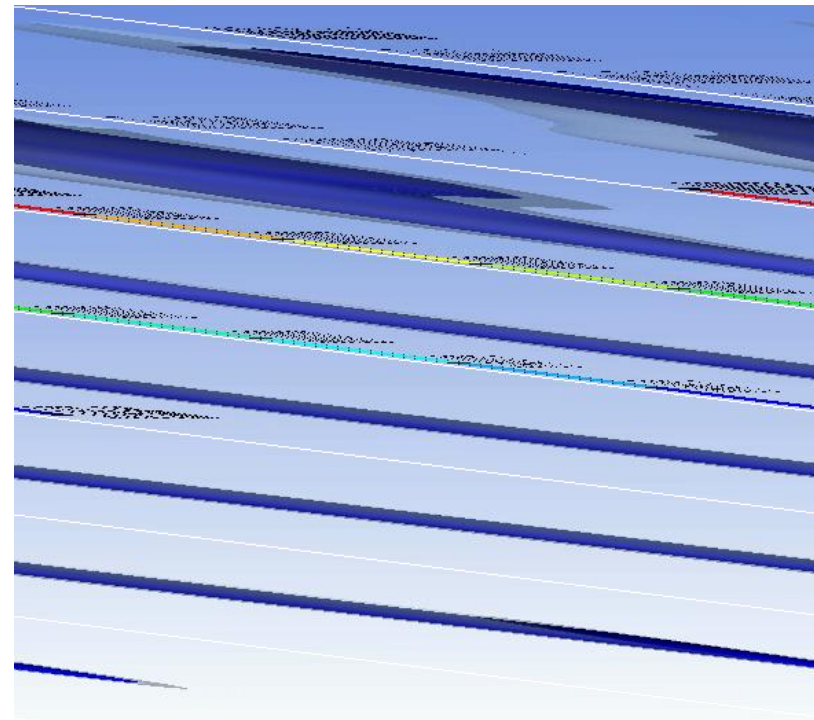




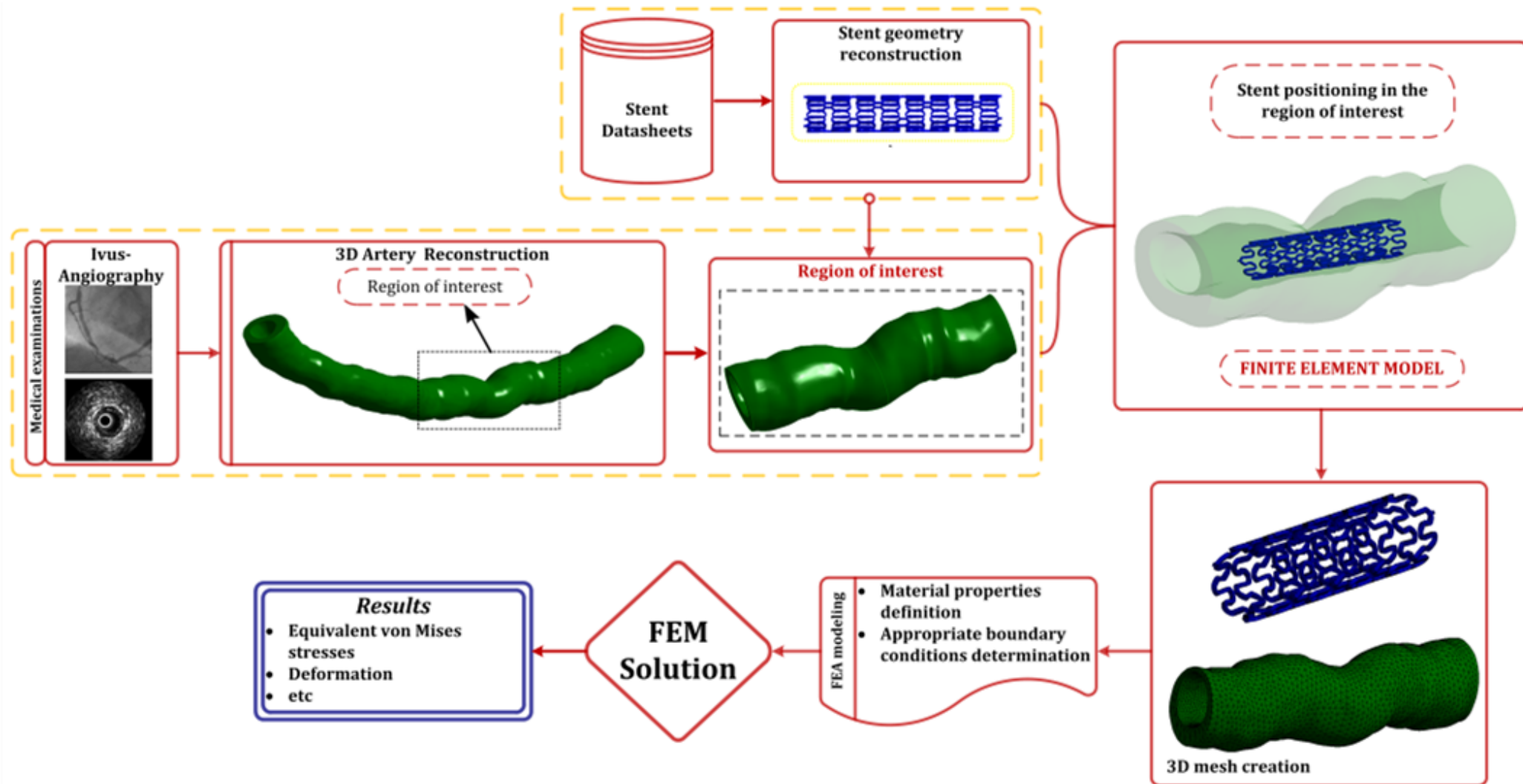
# Results



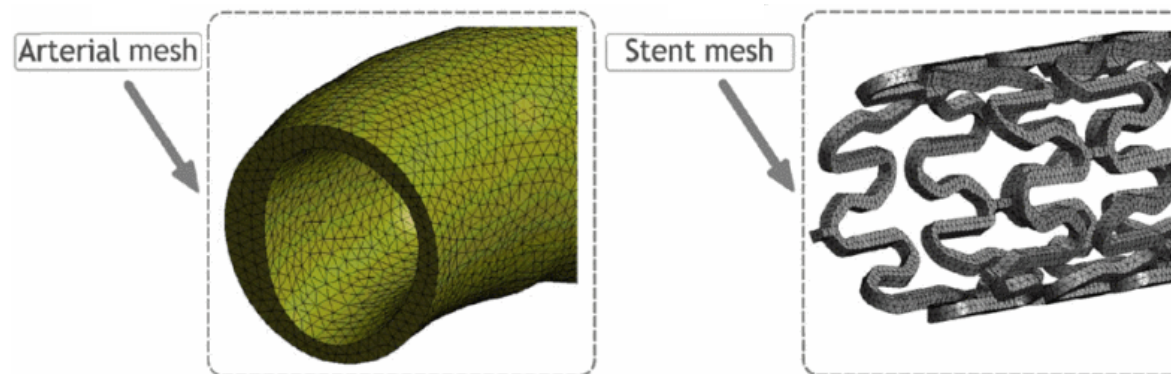
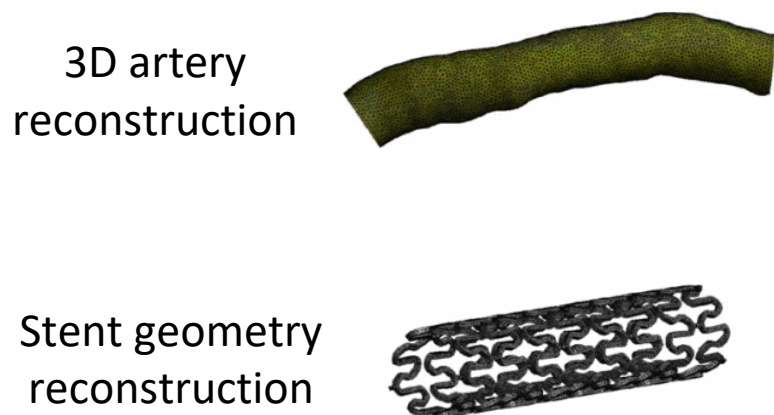
# Results



# Stent deployment modeling



# Stent deployment modeling



Arterial Geometry	Dimensional characteristics		
	Max Inner Diameter (mm)	Min Inner Diameter (mm)	Length (mm)
	4.40	2.26	30
Stent geometry	Inner diameter (mm)	Thickness (mm)	Number of rings
	1.26	0.081	8

Arterial Material Properties	Arterial hyperelastic coefficients				
	$C_{10}$	$C_{01}$	$C_{20}$	$C_{11}$	$C_{30}$
	0.0189	0.00275	0.08572	0.5904	0

Stent Material Properties			
	MODEL A	MODEL B	MODEL C
Elastic modulus (MPa)	232000	193000	200000
Yield strength (MPa)	414	360	355
Tensile strength (MPa)	738	675	834
Poisson's ratio	0.32	0.3	0.32

\* Tetrahedral lower-order 4-node elements (SOLID285) and higher order 10-node elements (SOLID187) were selected for the stent and artery mesh.



# Stent deployment modeling

- For all models, the curved areas of the stent links present higher stresses compared to the straight stent segments. The high stresses in these regions could indicate a risk for potential failure during stent expansion.

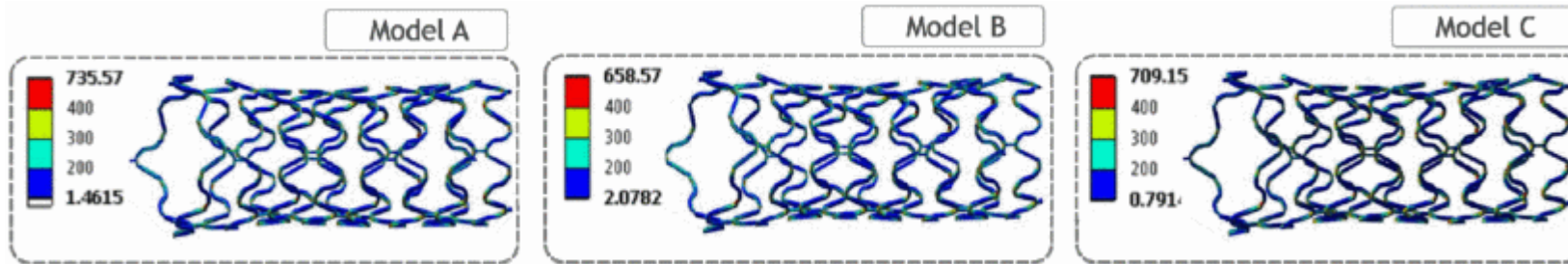


Fig. 1. The von Mises stress distribution. Maximum diameter achieved at 1.8MPa.

- After unloading, all stents followed a similar pattern of inner arterial stresses with maxi von Mises stresses at **0.65MPa** for **CoCr**, and **0.62MPa** for **SS** and **PtCr** stents.

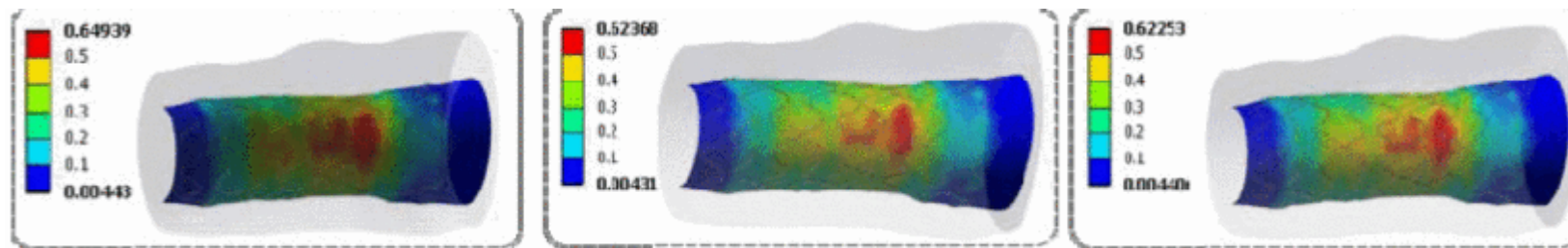
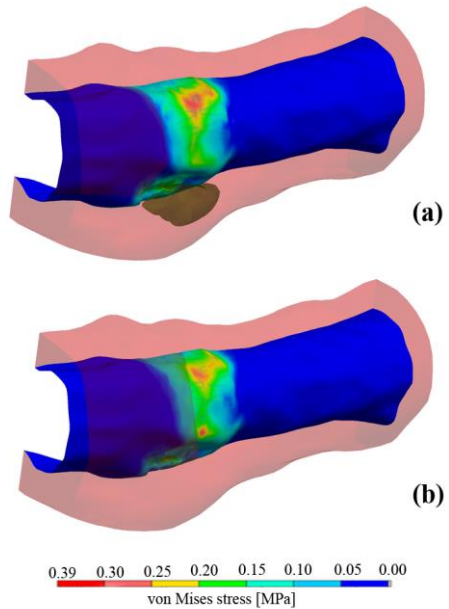
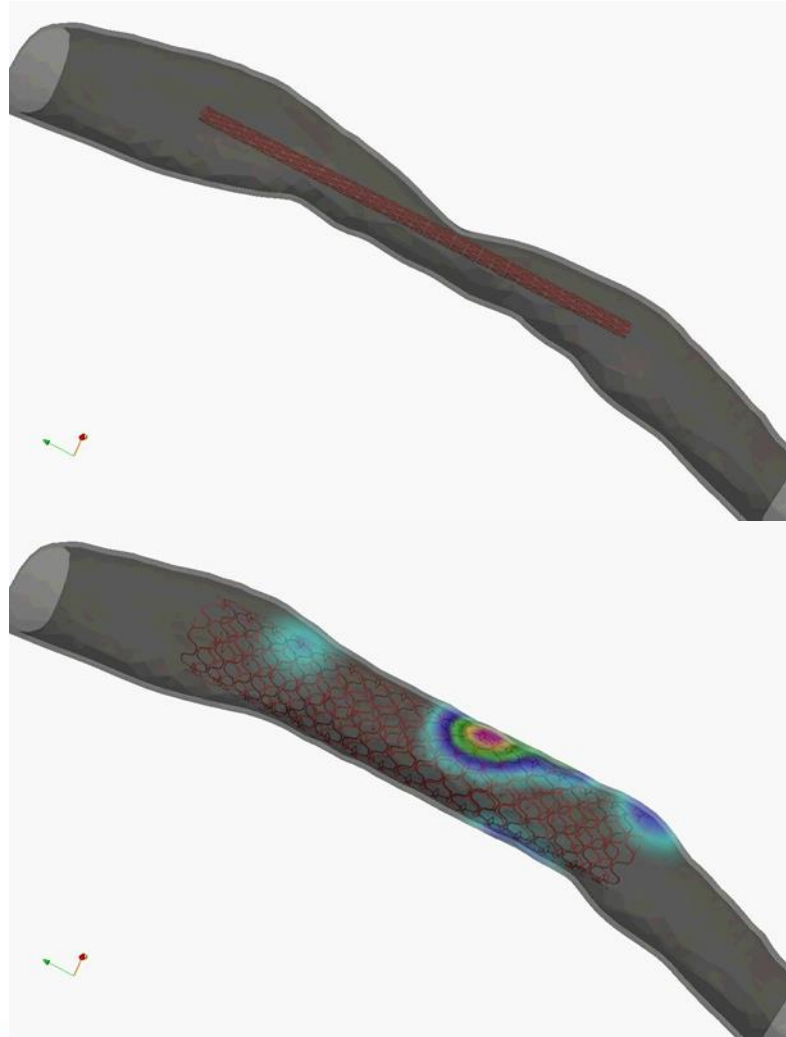


Fig. 2. The von Mises arterial stress after unloading

# Virtual stenting results



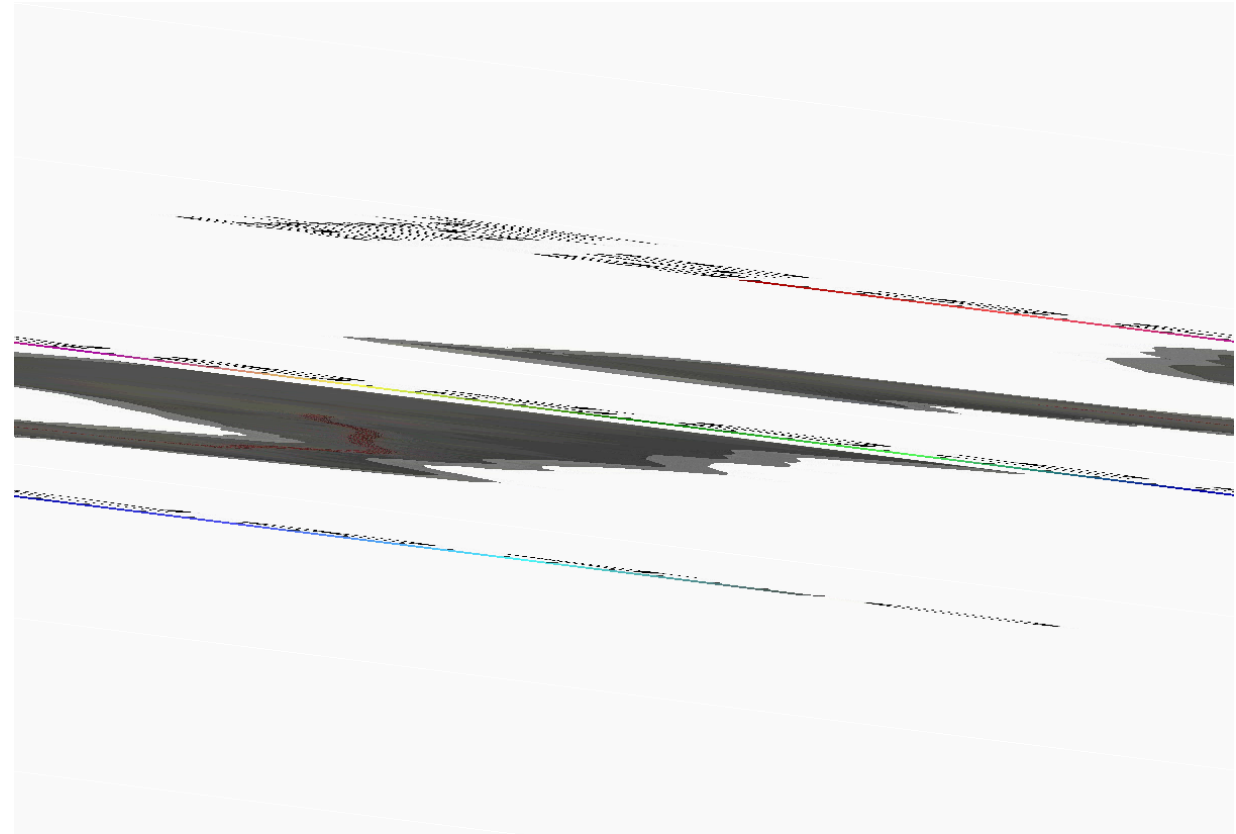
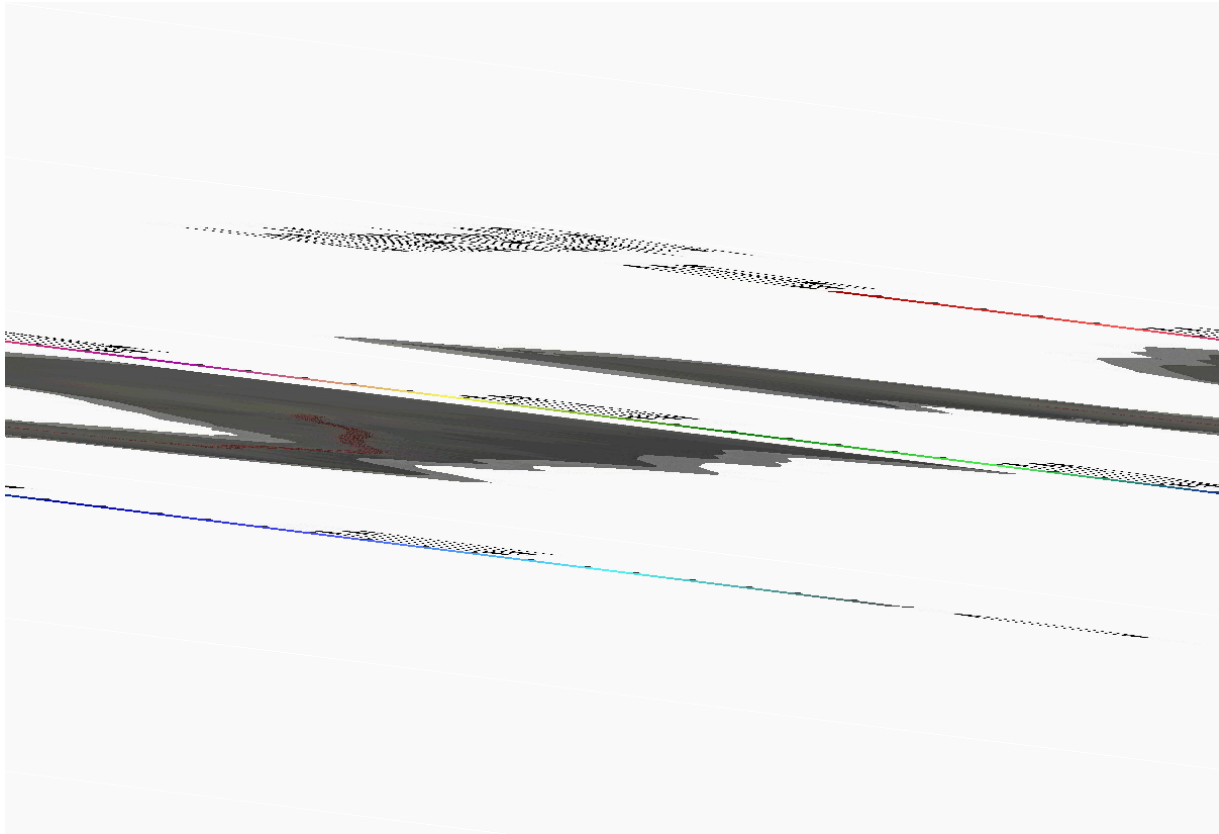
von Mises stresses for the models (a) with and (b) without the plaque component, respectively.



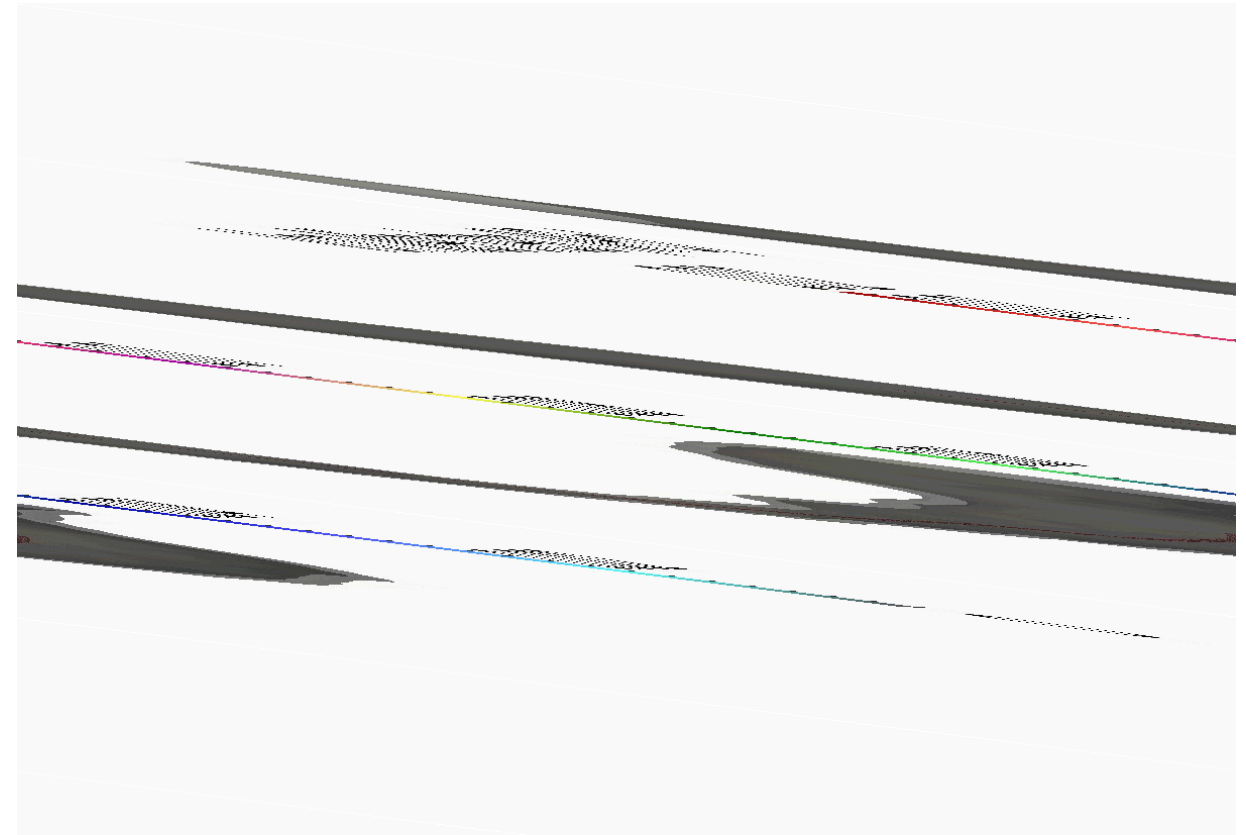
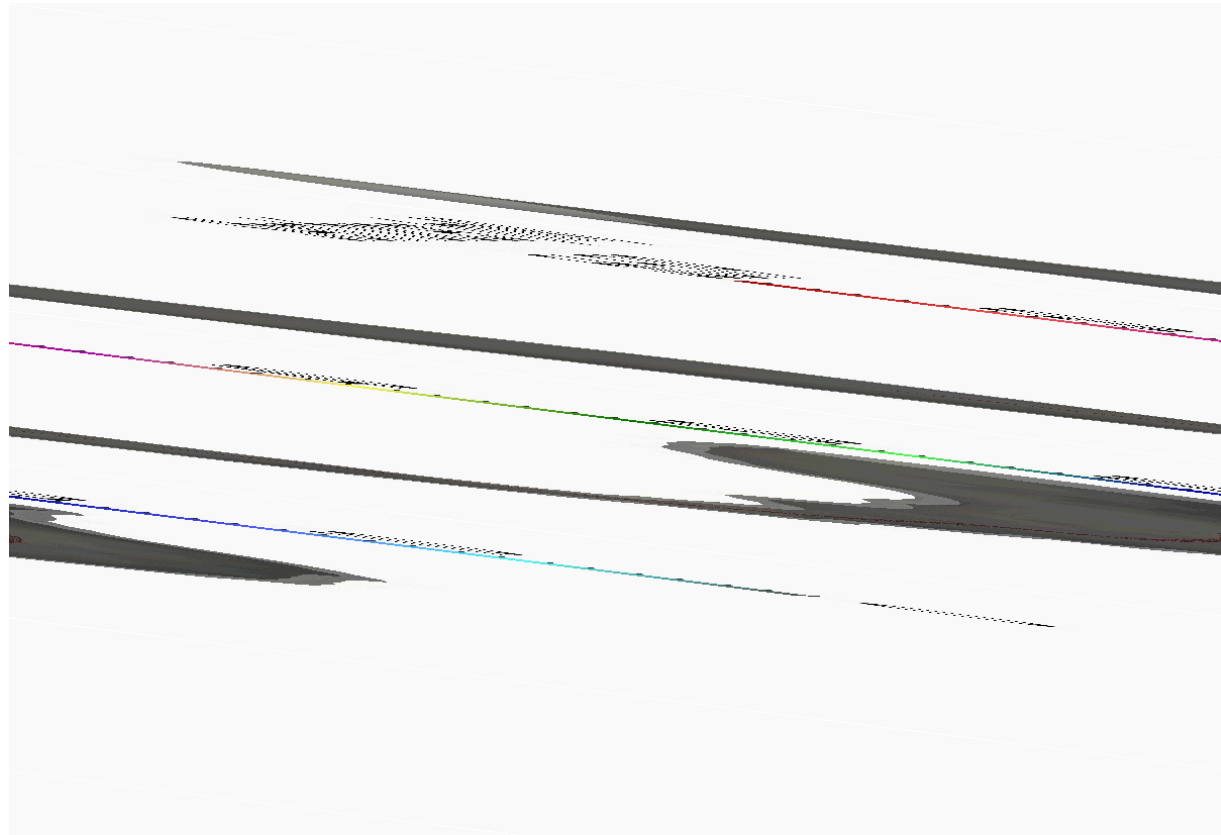
- Treatment decision support is provided by performing virtual stenting
- A novel FEM methodology provides fast and accurate simulation
- The proposed methodology is validated using SMARTool's data (pre- and post- stenting)



# Virtual stenting results



# Virtual stenting results



# Clinical use

SMARTool takes into account the **genotype** and **phenotype** of each individual in order to provide personalized diagnosis, prognosis and prediction of coronary heart disease.

1

A patient visits a practitioner/cardiologist and blood test is performed

The pre-imaging test of SMARTool provides a risk score

In case of high risk, the patient is going for CTCA

3

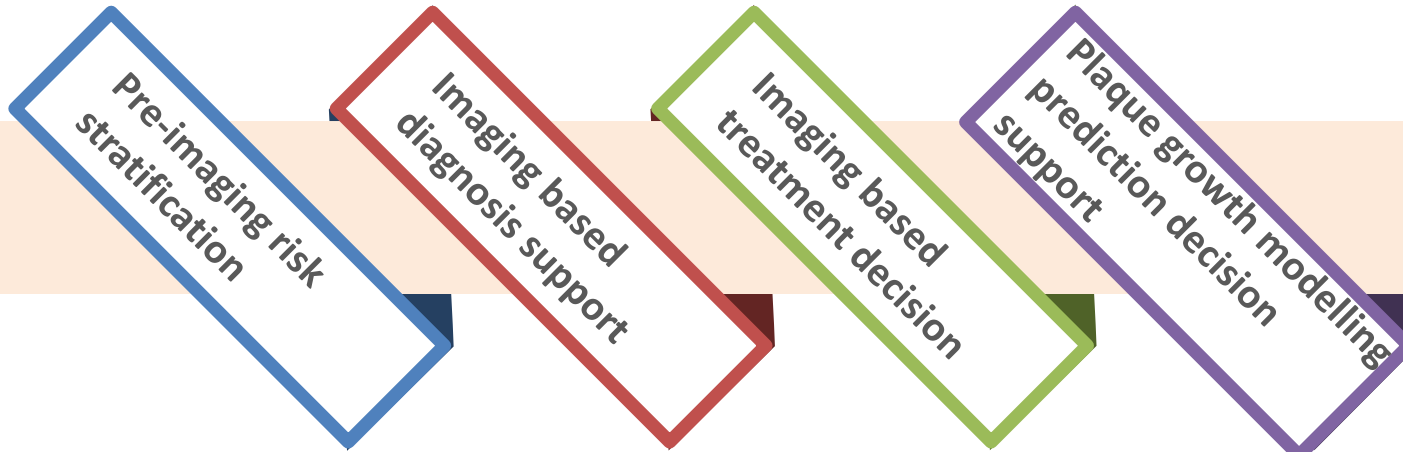
The arterial geometries are used for treatment decision support based on virtual stent deployment

2

The CTCA is used for 3D reconstruction and assessment of the atherosclerotic status  
The arterial geometries are used for diagnosis based on the SmartFFR

4

Plaque growth modelling results combined with the phenotype and genotype of each patient provides prediction of the atherosclerosis evolution based on advanced machine learning algorithms



# Challenges in diagnosis and prognosis of atherosclerosis

Harmonization of large cohorts.

Patient-centered multi-scale models

Personalized medicine

Inclusion of patient's environment info (social, diet, physical activity)



Accurate risk stratification

Detection of high risk regions of plaque progression

Use of patient's genetic profile in multi-scale models

SMARTool faces these challenges and provides decision support solutions for the risk stratification, diagnosis and prognosis of cardiovascular disease